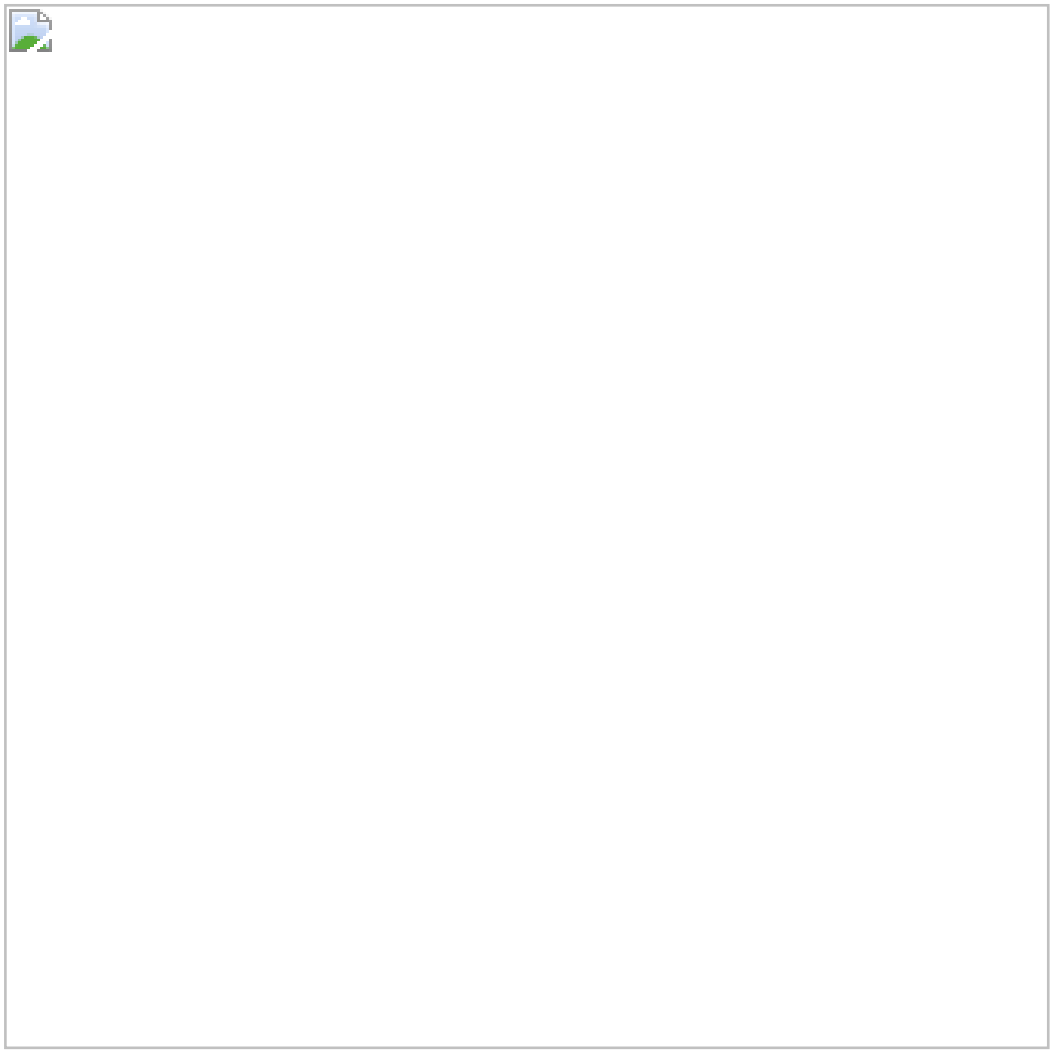

Assessment of the Relationship between Coastal Morphometry, Bottom Dynamic Conditions and the Critical Depth

Authors: Lindgren, Dan, and Karlsson, Magnus

Source: Air, Soil and Water Research, 4(1)

Published By: SAGE Publishing

URL: https://doi.org/10.1177/ASWR.S6918

Air, Soil and Water Research

ORIGINAL RESEARCH

Assessment of the Relationship between Coastal Morphometry, Bottom Dynamic Conditions and the Critical Depth

Dan Lindgren[1] and Magnus Karlsson[1,2]

[1]Department of Earth Sciences, Uppsala University, Villav. 16, SE-752 36 Uppsala, Sweden. [2]IVL Swedish Environmental Research Institute, P.O. Box 210 60, SE-100 31 Stockholm, Sweden.
Corresponding author email: dan.lindgren@geo.uu.se

Abstract: Coastal sediment can be classified by functional bottom type, depending on whether cohesive fine material is eroded (E), transported (T) or deposited/accumulated (A) there. The assessment of such bottom dynamic conditions is useful in many ways, including as a fundament for structuring mass balance models. In this paper more than 200 recently investigated Swedish coastal areas were analyzed using geographic information systems (GIS). Statistical relationships between morphometry, the average proportion of A-areas (BA) and the average critical depth (D_{TA}), which separates ET-areas from A-areas, were investigated. Many morphometric parameters showed significant correlation with both BA and D_{TA} and multiple regression models were obtained that could explain much of the variation in these parameters. Parameters describing sheltering effects from islands, mean depth and mean slope were important in this context. Large differences were found in empirical BA-values from two different sources. Furthermore, a new empirical dataset was presented for 209 Swedish coastal areas.

Keywords: coastal area, bottom dynamic conditions, sediment, critical depth, morphometry, GIS

Air, Soil and Water Research 2011:4 31–56

doi: 10.4137/ASWR.S6918

This article is available from http://www.la-press.com.

Introduction

Mass balance models and different types of budget calculations are important tools in coastal science and management to understand how coastal areas function and for prediction of the response to changes in pollution load and to different remedial measures.[1–5] Many pollutants and other substances have a high affinity for cohesive fine material[6,7] and when performing mass balance modeling it is thus vital to account for interactions between the water and the sediment.[8–12] Examples of such interactions are sedimentation and resuspension due to influence from waves. Waves displace sediment down to a certain depth and this depth varies with the wave height and wave length.[13,14] In mass balance modeling, and also other types of investigations, it is important to distinguish between bottom areas where cohesive fine material is continuously deposited and not eroded (accumulation areas, A) from bottom areas where the same material is continuously or discontinuously eroded (areas of erosion and transportation, ET).[15] The distribution of these different bottom types in a lake or coastal area is referred to as bottom dynamic conditions. Determination of bottom dynamic conditions and sediment types is also useful in mapping habitats for submersed vegetation, fish and other biota.[16–18] Determination of bottom dynamic conditions can be achieved using a side scan sonar, sediment echo sounder or multibeam echo sounder in combination with field sampling of sediment cores.[19–22] Different sediment types reflect the sound waves from the hydroacoustic devices differently. If the hydroacoustic equipment is linked to a navigational system, preliminary maps showing the distribution of different sediment types can be drawn. Sediment samples are collected for visual inspection and chemical analyses in order to confirm which of the functional sediment types is present. One method for establishing the functional sediment type is to analyze the content of water and organic matter in the upper layer; if these are above certain values, the sediment is considered A-sediment. According to Håkanson and Rosenberg,[23] a water content above 75% and/or a loss of ignition above 10% can be used as a rule of thumb to identify A-sediment in coastal areas. Field measurements of bottom dynamic conditions may produce accurate results, but require extensive and costly field work. Hence, any method that can estimate the distribution of different bottom types in a coastal area without having to perform field work would be useful.

The depth down to which waves displace cohesive fine sediment (the wave base) varies, both with time and with location within a coastal area. Periods with strong winds lower the wave base and decrease areas of accumulation. Conversely, during periods with calm weather the wave base is less deep than normal and sediment can be accumulated over larger areas than usual. However, for each location it is possible to identify a depth that over longer periods of time separates cohesive fine sediments affected by wave action (ET-areas) from sediments not affected by wave action[13] (A-areas). Such a depth can be averaged and identified for a whole lake or a whole coastal area and is then called the theoretical wave base (wb), or the critical depth[15] (D_{TA}). With a correct estimation of D_{TA} and an accurate bathymetric model, estimation of bottom dynamic conditions can be made with good precision. In mass balance modeling it has been shown to be useful to use the same depth for separating ET-areas from A-areas as for separation of surface water from deep water.[10,24] Thus the calculation or estimation of the critical depth and the wave base is an important part of mass balance modeling since it is a relevant separator of both sediment types and water masses in such models.

Håkanson and Jansson[15] estimated D_{TA} for whole lakes based on the surface water area (A), Eq. 1. This simplified approach is motivated because the maximum fetch is related to the surface area.

$$D_{TA} = \frac{45.7 \cdot \sqrt{A}}{\sqrt{A} + 21.4} \quad (1)$$

Eq. 1 was developed for lakes, and could possibly be applied to very enclosed coastal areas. In more open coastal areas the critical depth is not just a result of the fetch in the coastal area itself, but also of the fetch reaching the area from large adjacent basins or the sea. To be able to use Eq. 1 in more open coastal areas, Håkanson and Eklund[24] added exposure ($Ex = 100 \cdot At/A$; At = total cross sectional area) to the equation, Eq. 2. In that way they accounted for the fact that a high exposure (openness) lowers the wave base. Since the parameter in that investigation is a collective parameter used for both separation of

sediment types and water masses, it will be denoted wb also in this paper.

$$wb = \frac{45.7 \cdot \sqrt{A}}{\sqrt{A} + 21.4} \cdot \left(\frac{Ex}{0.003} \right)^{0.25} \quad (2)$$

From the definition of the different bottom types it is evident that the distribution of the E-, T- and A-bottom areas depends on waves and bathymetry, which determines the size of areas that are above/below the wave base. However, in addition to waves, bottom currents can also cause movement and resuspension of sediment below the wave base.[25] On slopes, less force is needed to move sediment and when slopes are really steep, very little influence is needed to induce erosion and transport of sediment. Thus, steep sloping areas can cause the occurrence of ET-areas below the wave base. The critical inclination above which this occurs depends on sediment characteristics like size.[26] According to Håkanson and Jansson[15] slope induced transport of cohesive fine sediment occur at slopes steeper than 4%–5%.

Previous efforts to predict bottom dynamic conditions of coastal areas using GIS and statistical methods include Persson and Håkanson[27] and Bekkby et al.[28,29] Brydsten[30] modeled bottom dynamic conditions in two large basins of the Baltic Sea using bathymetry and wind data. Studies of bottom dynamic conditions in the Baltic Sea, resuspension and the relation to waves were also performed by Jönsson et al.[31] Lindgren[32] investigated correlation between different morphometric parameters and bottom dynamic conditions with focus on openness and sheltering effects from islands. This paper will use a similar approach to Persson and Håkanson.[27] That investigation was based on data from 38 Baltic coastal areas while the current investigation extends to 69 Swedish coastal areas and includes several new morphometric parameters. A large data set of more than 200 Swedish coastal areas is also included, but with a more limited amount of morphometric data.

The overall aim of this work is to study bottom dynamic conditions and the critical depth as well as the factors affecting them. This will be achieved by first using GIS-based analysis to obtain morphometric properties of whole, well-delimited, coastal areas. Statistical analysis will then be used to investigate possible statistical relationships between these parameters, bottom dynamic conditions and the critical depth. The second aim is to find ways of estimating bottom dynamic conditions and the critical depth for whole, well delimited, coastal areas solely from morphometric parameters calculated from maps and sea charts.

Materials and Methods

Study areas and empirical data on bottom dynamic conditions

Empirical data on bottom dynamic conditions from 69 Swedish coastal areas[21,27] (referred to as focus areas) were used in the statistical analysis, Table 1, Figure 1A. The data in Persson and Håkanson[27] were obtained using a low frequency echo-sounder and surface sediment sampling while Jonsson et al[21] used a combination of side scan sonar, sediment echo sounder and navigational echo sounder in conjunction with sediment samples. Sediment map data based on empirical measurements (scale 1:100 000) were obtained from the marine geological map database of the Geological Survey of Sweden (SGU, © Sveriges geologiska undersökning). Those were analyzed and recalculated to bottom dynamic conditions for 209 coastal areas, Figure 1B. Of those areas, 202 had measurements covering at least 80% of each area (measurement cover) and 182 also had hypsographic data and were thus used in the statistical analysis. The sediment data from SGU were acquired using a combination of different hydro-acoustic measurements, different types of sediment sampling, video and highly detailed equipment for positioning.

Morphometric parameters

Based on previous studies[27,32] morphometric parameters that could possibly influence bottom dynamic conditions were selected for analysis (Table 2). More detailed descriptions of these parameters can be found in Persson and Håkanson,[27] Persson et al[33] and Lindgren.[32] Note that some parameter abbreviations agree with the more recent publications and may hence differ slightly from Persson and Håkanson.[27]

The filter factor (Ff) is a type of wave fetch index[34,35] that has shown correlation with bottom dynamic conditions in Swedish coastal areas.[27,32] Different simplifications of the filter factor were investigated by Lindgren[32] using a smaller dataset (n = 29). Here similar tests were performed using data

Table 1. Empirical data on bottom dynamic conditions from Persson and Håkanson[27] a) and Jonsson et al.[21] b). The numbers of the areas (the 'focus areas') correspond to the map in Figure 1.

Nr	Area	BA (%)	Source	Nr	Area	BA (%)	Source
1	Fabriksviken	7	a	36	Vaxholmsfjärden	33	b
2	Kylören	0	a	37	Älgöfjärd	48	b
3	Norrbyskär	28	a	38	Ö Saxarfjärden	58	b
4	Rönnskär	7	a	39	Himmerfjärden	21	b
5	Ångermanfjorden	71	b	40	Näslandsfjärden	49	b
6	Fälön	35	a	41	Stussviken	66	b
7	Hallstavik	56	a	42	Tväre n	59	b
8	Hargshamn	43	a	43	Aspöfjärden	32	b
9	Kallriga II	6	a	44	Bondekrok	34	b
10	Källsön	28	a	45	Dalvåmmen	42	b
11	Malören	34	a	46	Eknön	60*	b
12	Medholmen	40	a	47	Gropviken	51	b
13	Raggarön	28	a	48	Gräsmarö	40	a
14	Singöfjärden	32	b	49	Hålfjärden	27	b
15	Norrtäljeviken	38	b	50	Kullskärsdjupet	32	b
16	Baggensfjärden	45	b	51	Kärrfjärden	15	b
17	Bulleröfjärden	38	b	52	L. Rimmö	27	a
18	Edöfjärden	40	b	53	Lagnöströmmen	8	a
19	Erstaviken	45	b	54	Lindersfjärden	59	b
20	Farstaviken	39	b	55	Lönshuvudfjärden	29	b
21	Gälnan	51	b	56	Orren	38	b
22	Fj. S. om Vaxholm	36	b	57	Slätbaken	57	b
23	Kanholmsfjärden	47	b	58	Trännöfjärden	48	b
24	Norra Lilla Värtan	49	b	59	Ålö-Melö	6	a
25	Södra Lilla Värtan	45	b	60	Boköfjärd	4	a
26	Möja Söderfjärd	47	b	61	Guövik	35	a
27	Nassafjärden	42	b	62	Järnavik	0	a
28	Saltsjön	50	b	63	Matvik	0	a
29	Skagsfjärden	32	b	64	Ronneby	23	a
30	Skatfjärden	41	b	65	Spjutsö	2	a
31	Solöfjärden	79	b	66	Tärnö	0	a
32	Torsbyfjärden	50	b	67	Långökilen	6	a
33	Trälhavet	24	b	68	Starekilen	14	a
34	Träsköfjärden	39	b	69	Tjärnökilen	21	a
35	V Saxarfjärden	41	b				

Notes: *Value obtained by digitizing the map in Jonsson et al.[21]

from the 69 focus areas. Two other ways of describing openness and the sheltering effect from islands were tested by Lindgren[32] with good results. The first was the proportion of land (islands) in a 90° circle sector (InsO, %), aimed from the centre of the coastal area towards the sea. This parameter was also used in this study, with both 10 km and 30 km radius. The second parameter was created by spreading five points evenly across each coastal area and then calculating the total fetch by drawing a number of lines in all directions from each point. This parameter (denoted 5p) and a new variant, using 10 points per area and 256 lines around each point (denoted 10p) were used in this study. It was also desirable to test an approach where many points are evenly spread over the whole coastal area with lines drawn from each point. However, the computational demand of this approach was too high for the available hardware and was thus not possible.

In order to test whether a critical inclination could be found for the occurrence of slope induced erosion and transport all 69 focus areas were analyzed and the proportions of each area with a slope above 5% and 10% were calculated and used in the statistical analysis. These two inclinations were based on values from Håkanson and Jansson[15] and Rowan et al.[26]

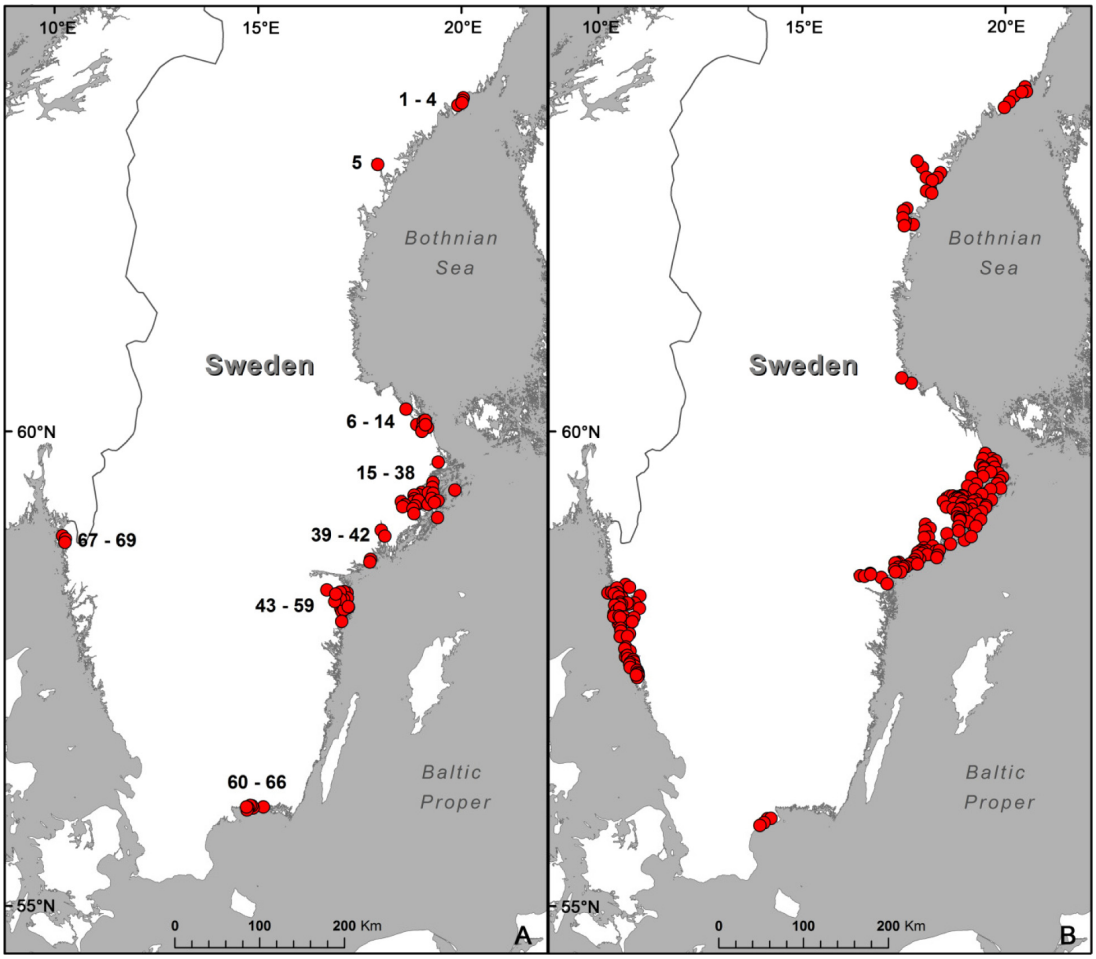

Figure 1. A) Location of areas with BA-data from Persson and Håkanson[27] and Jonsson et al,[21] n = 69; **B**) areas with BA-data available from SGU, n = 209.

The approach to calculate wb in Eq. 2 was used for comparison with estimates of D_{TA}. A second variant was also tested where the expression to lower the wave base was altered to adapt to the upper class limit of very enclosed areas suggested by Lindgren and Håkanson[36] (Ex = 0.02), which gives:

$$wb2 = \frac{45.7 \cdot \sqrt{A}}{\sqrt{A} + 21.4} \cdot \left(\frac{Ex}{0.02} \right)^{0.25} \quad (3)$$

These two wb variants and bathymetric data were then used to calculate the area under each wb variant (Awb, Awb2). Both the wb variants and the corresponding areas were included in the statistical analysis.

All morphometric parameters described were calculated, using ArcGIS 9.3, for the 69 focus areas in Table 1. Bathymetric information was digitized from navigational sea charts (scale 1:50 000) and digital coast line data with scale 1:50 000 were used for the Swedish coast (© Lantmäteriet Gävle 2011. Grant I 2011/0100). For calculation of fetch lengths off the Swedish coast, data from the Global Self-consistent, Hierarchical, High resolution Shoreline Database[37] (GSHHS) were used that have a working scale of 1:100 000 at best. The same boundaries were used as in the investigations from which the empirical bottom dynamic condition data emanate (maps available in Wallin et al,[38] Persson et al[33] and Jonsson et al[21]). It should be noted that some of the investigated areas in Jonsson et al[21] do not have boundaries drawn at sills or bathymetric ridges.

Evaluation of empirical bottom dynamic condition data

It is difficult to assess the uncertainty of empirical BA-values since the values result from a complex

Table 2. Investigated morphometric parameters. For detailed descriptions see Persson and Håkanson[27] and Lindgren.[32]

Type	Parameter	Unit	Description
Length	l	km	Coastal length
Length	L	km	Total shore length
Length	P	km	Perimeter
Length	W	km	Mean width
Area/volume	Atot	km^2	Total area (both water and islands)
Area/volume	A	km^2	Water surface area
Area/volume	Ab	km^2	3-dimensional bottom area
Area/volume	Ab3	km^2	Bottom area above 3 m
Area/volume	Au3	km^2	Bottom area below 3 m
Area/volume	V	km^3	Water volume
Depth	Dm	m	Mean depth
Depth	O10 m	m	Mean depth below 10 m
Depth	Dmax	m	Maximum depth
Form/shape	Vd		Form factor, volume development = 3 · Dm/Dmax
Form/shape	DR		Dynamic ratio, relative depth = Sqrt(A)/Dm
Form/shape	xm	%	Mean slope
Form/shape	xm5	%	Proportion of areas with a slope >5%
Form/shape	xm10	%	Proportion of areas with a slope >10%
Islands	Ai	km^2	Area of enclosed islands
Islands	Im	km^2	Mean size of islands
Islands	Ins	%	Insulocity, proportion of islands
Islands	li	km	Island shore length
Islands	N		Number of enclosed islands
Wave base	wb	m	Critical depth/theoretical wave base, as in Eq. 2
Wave base	wb2	m	Critical depth/theoretical wave base, as in Eq. 3
Wave base	Owb	m	Mean depth under wb
Wave base	Owb2	m	Mean depth under wb2
Wave base	Awb	km^2	Bottom area under wb
Wave base	Awb2	km^2	Bottom area under wb2
Openness	Op	%	Proportion of boundary that consists of water (sounds)
Openness	At	km^2	Total cross sectional area (of all boundary sounds)
Openness	n		Number of openings/sounds
Openness	n10		Number of openings with a sill depth >10 m
Openness	n100		Number of openings with a cross sectional area >100 m^2
Openness	Ex		Exposure (= 100·At/A)
Openness	Ff	km^3	Filter factor
Openness	MFf		Mean filter factor (= Ff/n)
Openness	FfL	km	Summed length of filter factor lines
Openness	5p	m	5-point filter factor alternative
Openness	10p	m	10-point filter factor alternative, similar to 5p
Openness	InsO 10 km	%	Proportion of islands in a circle sector outside, r = 10 km
Openness	InsO 30 km	%	Proportion of islands in a circle sector outside, r = 30 km

multi-step process, which to some degree includes human judgment. However, for 33 of the focus areas in Table 1 sediment maps were also available from a second source (the SGU). Hence, values of bottom dynamic conditions (BA, %) were calculated using the maps from SGU and these new data were compared with the corresponding values in Table 1 to obtain an estimate of the uncertainty in empirical BA-data.

Derivation of statistical bottom dynamic condition models

The statistical analyses that were performed include simple linear correlation and (forward stepwise) multiple regression. These are both relatively simple statistical standard methods and hence the theory behind these is not explained here in detail, although some considerations are discussed. For more information about background theory and the advice and practices

followed, please refer to, eg, Ryan,[39,40] Weisberg[41] and Rubin.[42] Stability tests were also performed as described by Håkanson and Peters,[43] who discussed many practical considerations and provided good advice on the subject. The statistical software Statistica was used for all statistical analysis.

When performing linear regression and stepwise multiple regression (SMR), some assumptions and requirements need to be met. One of the more important is that the included parameters need to be normally distributed.[42–44] Other assumptions include that the error terms (residuals) should also be normally distributed and independent.[40] The frequency distributions of all parameters were hence first checked for normality by investigating the histograms (with additional support from normality tests) and those not normally distributed were transformed. The variants that were most normally distributed were then used in the statistical analysis. Correlation between each parameter and BA was tested and SMR was then used to obtain statistical models with BA as target (dependent) parameter and all morphometric parameters as independent variables. Residual analysis was performed to ensure that the other assumptions were met. The outcome of a SMR is dependent on the range of the included variables and one, or a few, outliers can alter the result significantly. An outlier is an observation that deviates clearly from the rest of the sample in which it occurs. What is considered a clear deviation is subjective and may vary from investigation to investigation. When studying coastal areas with many properties using multiple regression the definition becomes more complex. One way of defining outliers is by using the "three-sigma rule" stating that for a normal distribution nearly all values (≈99.7%) lie within 3 standard deviations (3σ) of the mean. If n is not very small, this rule can be used in multiple regression by looking at the standardized residuals and cases with standardized residuals $> 3\sigma$ can be considered outliers.[45] The dataset was hence searched for outliers, both in the raw data, but also using residual analysis. Finally, the models were tested using a type of stability test[43] where a random selection of coastal areas (here about 10% ≈7) were removed repeatedly (10 times). Each time a new SMR-model was calculated and differences in r^2-value, intercept and model coefficients were studied.

The inclusion of several parameters in the SMR model that are too internally correlated (multicollinearity) may make it difficult to find causal interpretations of the obtained model and in extreme cases it may cause errors in the analysis.[39,40,42] Hence, internal correlation among the model parameters was investigated using an r-rank matrix. The choice of r-value to use as a cutoff point is a difficult decision. The limit for belonging to the same cluster ($r = 0.5$)[43] is too strict to be used in this context. According to Rubin[42] the cutoff point when multicollinearity becomes a problem varies and can be set at, eg, $r = 0.60$, 0.80 or even 0.90. Rubin recommended exclusion of a parameter if $r > 0.90$, but here $r = 0.75$ was used. In this way inclusion of redundant variables was avoided.

The statistical analysis described above was first performed on the 69 focus areas. For 33 of these areas, BA-values were available from two sources (Persson and Håkanson[27] or Jonsson et al[21] and SGU) and for those areas mean values were used. It would certainly be valuable if it were possible to obtain an estimate of bottom dynamic conditions using only very simple and widely available parameters, ie, without having to perform extensive GIS analysis first. In an attempt to explore this, BA was calculated for the 202 coastal areas with at least 80% measurement cover, based on the maps from SGU. For this the boundaries used in the Swedish Sea Registry[46,47] were applied. For these areas the following morphometric parameters are available in the Sea Registry: A, V, Dm, Dmax and At. From these parameters some other simple parameters, like Vd and DR, could also be calculated. This much larger dataset, with a limited number of morphometric parameters, was used in a similar statistical analysis to that described in the previous section.

Approximation of the critical depth

Using empirical data on bottom dynamic conditions and hypsographs, created from bathymetric data, it is possible to calculate an empirical estimate of the critical depth, D_{TA}. This estimate is then defined as the depth under which the area is equal to the measured area of accumulation, assuming that all A-areas are situated on the deepest bottoms. The calculation of D_{TA} was done for the 69 focus areas and for 201 of the SGU areas where hypsographs from SMHI[48] were also available. The two wb-variants (Eq. 2 and Eq. 3) were also calculated for all coastal areas

and compared with the values of D_{TA} using linear regression. All parameters were checked for normality before analysis and transformed where necessary. The morphometric data and D_{TA}-values calculated from empirical data were used to obtain a new statistical model of D_{TA} using SMR. The procedure was the same as previously described.

Håkanson[49] presented an algorithm for calculation of the area under the wave base in lakes based on the hypsographic shape, using the parameters A, Dmax and Vd, Eq. 4. Lindgren[50] investigated whether that algorithm could also be used for coastal areas and when comparing the calculated values with values calculated from real hypsographs for 541 Swedish coastal areas an r^2-value of 0.87 was obtained. If an estimate of D_{TA} can be calculated for a coastal area and no hypsographs are available, this equation may be used to obtain an estimate of BA. In this study it was used for comparison with the area values obtained by the real hypsographs for the 201 coastal areas.

$$A_{below\,wb} = A \cdot \left(\frac{D_{\max} - D_{wb}}{D_{\max} + D_{wb} \cdot \exp(3 - Vd^{1.5})} \right)^{0.5/Vd} \quad (4)$$

Results

Morphometric data

Basic statistics for the morphometric parameters from the 69 focus areas are presented in Table 3 and the corresponding statistics for the morphometric parameters available in the extended dataset are presented in Table 4. Note that the former are based on data obtained using GIS-analysis while the latter are based on data from the Swedish Sea Registry. Tables 3 and 4 show that in many cases the range of parameter values in the focus areas is not much less than in the large dataset.

Evaluation of empirical bottom dynamic condition data

The sediment data from SGU enabled calculation of BA for 209 areas in total, Figure 2. These values may be of use in other scientific studies and are thus presented in Appendix A. The mean value of BA among all 209 areas is 27% and the corresponding median is 24%. Figure 2 shows that about 25% of the areas have a very low proportion of accumulation areas (BA $<$ 5%). Above this value the distribution is quite even up to about BA = 55%. The results from the spatial analysis displayed in Figure 3 show that areas with low BA-values are generally unsheltered and situated further out on the coast, while coastal areas with higher BA are mostly sheltered. This indicates that exposure to waves and the presence or absence of sheltering islands may be of importance for the bottom dynamic conditions in the investigated areas. Note that the boundaries of the focus areas were drawn according to the original sources, while the areas in Appendix A use boundaries from the Swedish Sea Registry.

The comparison of empirical BA-values from different sources, with exactly the same boundaries, shows quite remarkable differences, Table 5, yielding low correlation ($r^2 = 0.22$). It was investigated whether any morphometric properties cause greater differences in the empirical values by trying to find correlation between the (transformed) CV values (CV = standard deviation/mean) and all other parameters. A significant correlation was found between the number of islands within the area (N) and CV ($r = 0.37$; $P < 0.05$; $n = 33$), ie, the two measurements of BA differ more in areas with many islands. The reason for this may be that the measurement process is more complicated in areas with many islands. Insulocity outside (InsO) showed a significant negative correlation with CV ($r = -0.41$; $P < 0.05$, $n = 33$), meaning that the more sheltered an area is, the smaller the difference between the data from the two sources. Considering the great differences between the empirical sources, mean values were used for the areas with more than one value in the following statistical analysis.

Statistical models of bottom dynamic conditions

The results of the linear correlation between the different morphometric parameters and the proportion of accumulation bottom areas (BA) are shown in Table 6. Here, only the parameters that show significant correlation ($P < 0.05$; $n = 69$) have been included and only the parameter variant with best correlation. Many of the parameters that are related to the different wave base approximations show high correlation with BA, which indicates that these approximations work quite well. Simple parameters like mean depth (Dm) and maximum depth (Dmax) also show high

Table 3. Basic statistics for the morphometric parameters calculated for all 69 focus areas.

Type	Parameter (unit)	Min	Median	Mean	Max
Length	l (km)	3.3	23.5	27.5	71.1
Length	L (km)	3.3	33.9	43.3	221.1
Length	P (km)	4.4	27.3	31.0	77.9
Length	W (km)	98.5	361.1	450.2	2806.1
Area/volume	Atot (km^2)	0.5	8.8	13.2	48.7
Area/volume	A (km^2)	0.5	8.3	12.6	46.8
Area/volume	Ab (km^2)	0.5	8.2	12.4	46.6
Area/volume	Ab3 (km^2)	0.1	1.4	1.9	9.5
Area/volume	Au3 (km^2)	0.4	6.5	10.4	40.1
Area/volume	V (km^3)	0.003	0.08	0.20	1.26
Depth	Dm (m)	2.2	9.5	13.0	56.0
Depth	O10 (m)	10.0	14.6	18.7	59.6
Depth	Dmax (m)	7.1	30.6	36.6	107.7
Form/shape	Vd	0.5	1.0	1.1	1.8
Form/shape	DR	0.1	0.3	0.3	1.1
Form/shape	xm (%)	1.2	5.3	5.7	13.3
Form/shape	xm5 (%)	3.5	34.4	34.6	73.7
Form/shape	xm10 (%)	0.4	12.4	15.0	46.6
Islands	Ai (km^2)	0	0.2	0.6	4.5
Islands	Im	0	0.02	0.06	0.45
Islands	Ins (%)	0	2.7	3.9	21.4
Islands	li (km)	0	6.2	15.9	169.1
Islands	N	0	23	52.7	674
Wave base	wb (m)	2.9	14.1	16.6	39.6
Wave base	wb2 (m)	1.8	8.8	10.4	24.6
Wave base	Owb (m)	7.6	19.5	23.4	73.7
Wave base	Owb2 (m)	5.7	15.7	19.3	66.2
Wave base	Awb (km^2)	0.002	1.0	3.1	23.2
Wave base	Awb2 (km^2)	0.2	3.4	5.4	25.5
Openness	Op (%)	1.1	9.3	12.7	58.3
Openness	At (km^2)	0.0002	0.014	0.037	0.401
Openness	n	1	9	14.7	69
Openness	n10	0	3	3.5	20
Openness	n100	1	7	9.2	36
Openness	Ex	0.020	0.2	0.3	2.4
Openness	Ff	0.008	7.6	67.4	1665.3
Openness	MFf	0.01	0.8	6.0	109.0
Openness	FfL	0.1	2	17.5	228
Openness	5p (m)	3.9E+05	2.4E+06	3.8E+06	2.4E+07
Openness	10p (m)	6.7E+05	4.6E+06	7.1E+06	4.1E+07
Openness	InsO 10 km (%)	0.2	25.7	30.4	82.0
Openness	InsO 30 km (%)	0.1	8.1	16.2	71.0

correlation. This is a useful result since these parameters are available for all Swedish coastal areas in the Swedish Sea Registry.

The tests of the filter factor showed that the best correlation with BA is obtained using a line length of 400 km and when using only openings with a cross sectional area over 100 m^2 for MFf. A slightly lower correlation was found when the number of lines was reduced. The total filter factor length (FfL) shows higher correlation than both the filter factor and the mean filter factor. When only addressing the linear correlation with BA, the best filter factor variant (MFf, max length 400 km, opening size >100 m^2) showed slightly better correlation ($r = -0.43$) than the best 5 point alternative (5 points, 256 lines, max length 100 km; $r = -0.39$). Although the 10-point filter factor alternative should give a more detailed representation of the area, compared to its 5-point counterpart, it does not yield higher correlation with BA. The other filter factor alternative, insulocity outside (InsO, %),

Table 4. Basic statistics of the extended SGU data set (n = 182).

Parameter	Min	Median	Mean	Max
A (km^2)	1	13	27	266
At (km^2)	0.0001	0.024	0.066	1.11
Ex	0.0036	0.19	0.26	1.30
V (km^3)	0.01	0.1	0.4	10.2
Dm (m)	1	9	11	52
Dmax (m)	3	34	39	116
Vd	0.3	0.9	0.9	2.8
DR	0.1	0.4	0.6	3.7

showed the highest individual correlation with BA and performed better using a sector with r = 10 km instead of 30 km. In the study of the effect of slope it can be noted that the proportion of areas with a slope > 5% (xm5) showed slightly better correlation with BA than the corresponding parameter based on 10% and that both showed clearly better correlation than mean slope (xm).

Table 7 shows the results from the first stepwise multiple regression analysis. The final model yielded an $r^2 = 0.74$ which is above the limit for what can be considered practically useful in coastal management (r^2-value > 0.65–0.70).[43,51] A higher InsO (%), ie, more sheltering islands outside the area, results in less influence from waves and a higher BA. Compared with other, more complex, descriptors of openness like the filter factor (Ff) and mean filter factor (MFf), calculation of InsO does not need bathymetric data. Inclusion of mean depth (Dm) is explained by shallow coastal areas on average being more affected by wave action, and hence having more ET-areas (and thus lower BA). Deep coastal areas also have a larger sediment trapping capacity.[21] A higher average slope means larger areas with gravitationally induced sediment transport (ET-areas), but at the same time steeper slopes are more prevalent in coastal areas with larger mean depths (the two show a positive correlation), which has the opposite effect. The last included parameter (5p) is a descriptor of openness and a higher value (more open) would increase the effect from waves and thus give a lower BA. The changed sign for xm from Table 6 to Table 7 is most likely not an error, but a result of partial internal correlation as will be discussed. However, when xm (and variants thereof) were excluded from the analysis the best model was: $BA = 4.4 \cdot \mathrm{sqrt}(InsO) + 8.4 \cdot \ln(Dm) + 2.9 \cdot \ln(Au3) - 54.0$. Here the area below 3 m (Au3, m^2, ln-transformed) entered the model instead in the third step and the total r^2-value was 0.67. Another option when parameters are internally correlated is to

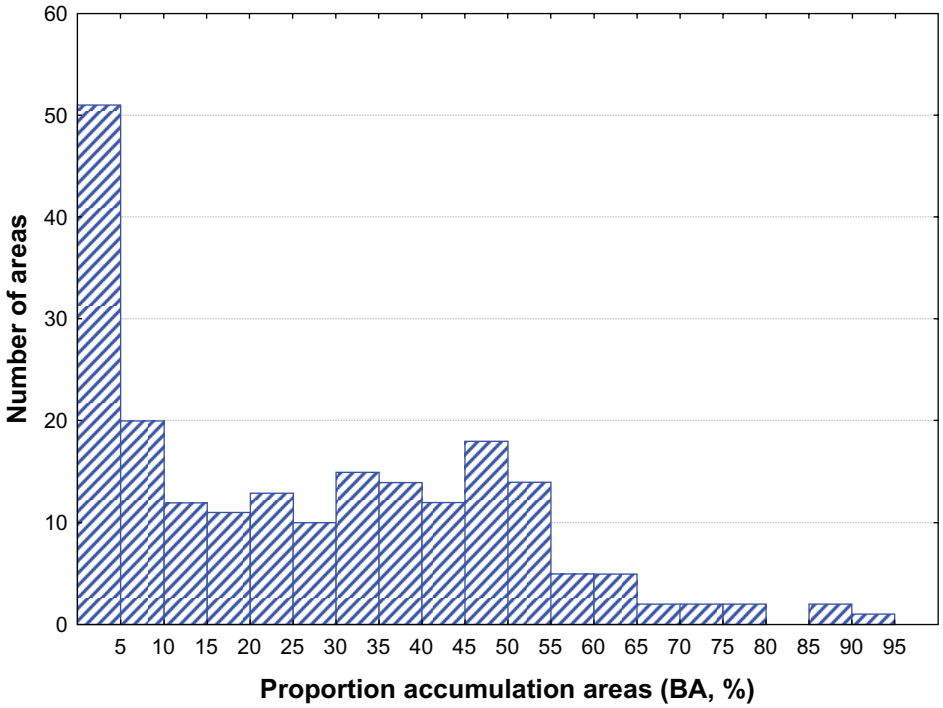

Figure 2. Distribution of BA values among 209 Swedish coastal areas.

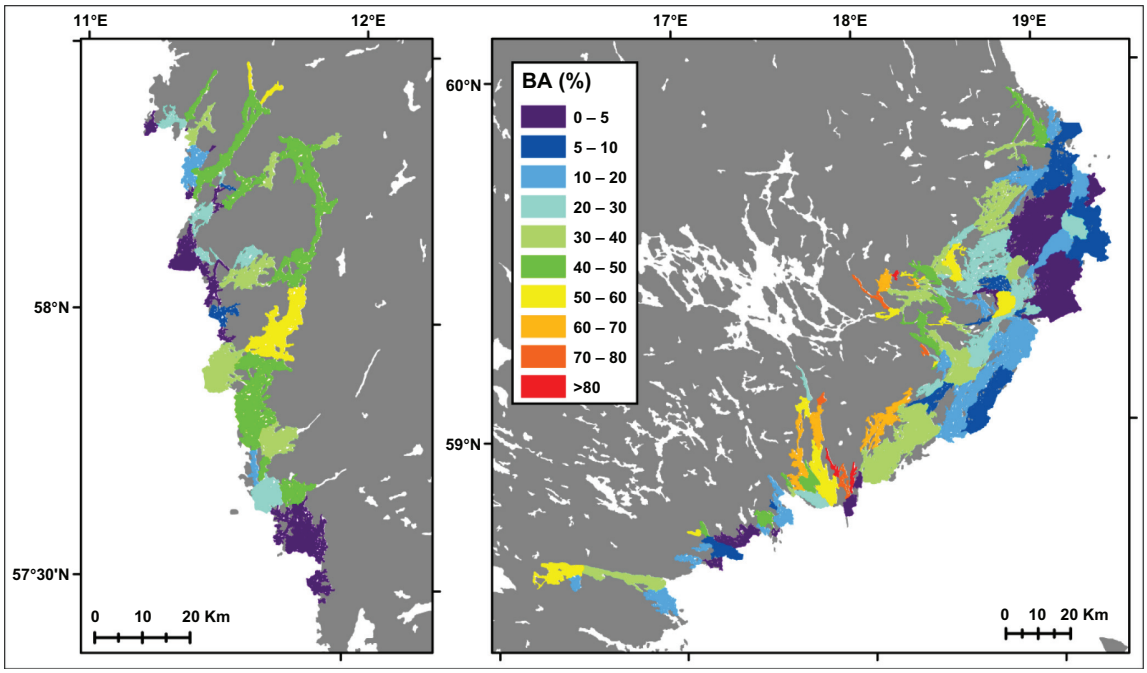

Figure 3. Maps showing BA-values (%) for some Swedish coastal areas.

combine the two into one new parameter.[42] This was tried by combining Dm and xm in different ways. The best model using this option obtained an $r^2 = 0.70$ with InsO selected first, then the Dm/xm-index and finally MFf. When only the 33 empirical data from the most recent measurements (SGU) were used, a model with $r^2 = 0.80$ was obtained in three steps ($F > 4$) with InsO, Ab3 (bottom area shallower than 3 m) and xm as parameters. Ab3 entered the model instead of Dm, but the two are highly correlated ($r = -0.95$).

Figure 4 shows values of BA calculated using the model in Table 7 (BAmod) and using the model where Au3 replaced xm (BAmod2) versus empirical BA-values. This shows that for the areas with BA = 0, both models predict values that are too high. The first model (BAmod) also predicts one negative value (excluded from the figure), which naturally is not realistic.

The residual analysis of the model for the 69 focus areas identified three areas with a standardized residual just above 2σ (Hallstavik, Guövik and Lagnöströmmen). These are all from the oldest and least reliable dataset, none of them are based on more than one value and they are all shallower than the average of all areas. Studying residuals and standardized residuals showed no evidence of non-normality or dependence.

The result of the stability test involving removing 7 random areas (≈10%) 10 times is presented in Table 8. In such a test smaller CV values indicate a more stable model. Table 8 shows that the intercept and the last parameter (5p) vary to some extent (CV = 0.2), while the other model coefficients are fairly stable. The order of the model parameters is also always the same. Based on this, the overall interpretation of the stability test is that the model is quite stable.

Approximation of the critical depth

The approach used to calculate an estimated value of the critical depth from bathymetry and empirical values of BA seems to work quite well, since the areal extent of the areas below D_{TA} in most cases coincides well with the empirical map of A-bottom areas, see examples in Figure 5. When studying the map data it was evident that ET-areas were sometimes also present in deep areas, ie, below the critical depth. Slope maps obtained from bathymetry showed that a steep slope is sometimes, but not always, the cause of such occurrences. Since the total area under D_{TA} is equal to the empirical value of A-areas, observations of ET-areas under D_{TA} were always accompanied by A-areas above the critical depth, eg, in local bays or deep holes. Table 9 displays the morphometric parameters showing the highest linear correlation with the estimated

Table 5. Differences in empirical BA-values.

Area	BA (%) Persson/ Jonsson	BA (%) SGU	Abs Diff (%-units)
Solöfjärden	79	25.2	53.8
Himmerfjärden	21	63.4	42.4
Stussviken	66	24.2	41.8
Nassafjärden	42	7.0	35.0
Älgöfjärd	48	14.6	33.4
Norrbyskär	28	0	28.0
Norra Lilla Värtan	49	75.6	26.6
Skagsfjärden	32	8.2	23.8
Gälnan	51	27.9	23.1
Norrtäljeviken	38	55.0	17.0
Trälhavet	24	40.9	16.9
Ångermanfjorden	71	55.2	15.8
Bulleröfjärden	38	23.5	14.5
Tväären	59	46.4	12.6
Edöfjärden	40	29.3	10.7
Träsköfjärden	39	29.2	9.8
Möja Söderfjärd	47	37.7	9.3
Kanholmsfjärden	47	56.0	9.0
Södra Lilla Värtan	45	52.9	7.9
Fjärdarna s. Vaxh.	36	28.2	7.8
Farstaviken	39	31.8	7.2
Fabriksviken	7	0	7.0
Rönnskär	7	0	7.0
Torsbyfjärden	50	44.7	5.3
Saltsjön	50	53.8	3.8
Östra Saxarfjärden	58	54.5	3.5
Baggensfjärden	45	42.2	2.8
Skatfjärden	41	38.3	2.7
Västra Saxarfjärden	41	43.2	2.2
Näslandsfjärden	49	50.2	1.2
Erstaviken	45	46.2	1.2
Vaxholmsfjärden	33	33.1	0.1
Kylören	0	0	0.0
Max	**79**	**75.6**	**53.8**
Mean	**41.4**	**34.4**	**14.7**
Median	**42.0**	**37.7**	**9.3**
Min	**0**	**0**	**0**

D_{TA} (ln-transformed). The mean depth (Dm) and the mean depth under the two wb-variants all show high correlation.

The best multiple regression model was: $\ln(D_{TA}) = 0.64 \cdot \ln(Dm) + 0.065 \cdot \ln(Ff) + 0.96$, ($F > 4$ in all steps). This model gave a relatively high r^2-value (0.78) and could possibly be used for estimation of the critical depth for use in, eg, mass balance modeling. The inclusion of mean depth (Dm) is expected because it is a simple descriptor of bathymetry and the empirical estimates of D_{TA} were obtained using hypsographs and empirical BA-values. A higher filter factor value (Ff) means a more open area, more waves coming in and thus a deeper (larger) critical depth. Residual analysis confirmed that the underlying assumptions of the SMR were fulfilled. No outliers ($>3\sigma$) were identified, but there were three cases with a standardized residual between 2–3σ. These areas (Hallstavik, Hargshamn and Lagnöströmmen) are all from the oldest, and most uncertain, dataset and are also all rather shallow. The result of the stability test, (removing ≈10% = 7 random areas 10 times), Table 10, shows that the model is more stable for changes of ln(Dm) than of ln(Ff), but all CV-values are low.

The results of comparing the two approaches to calculate wb for coastal areas (wb and wb2) with the modeled D_{TA} (D_{TA}mod) and the critical depth estimated from empirical BA and bathymetry (D_{TA}), are displayed in Figure 6. Here wb is on average 23% larger (ie, deeper) than D_{TA} and wb2 is on average 23% smaller than D_{TA}. When studying the effect from the different wb approximations on BA, wb gives a total accumulation bottom area that is 32% smaller than the measured BA. The modified version, wb2, conversely gives a 20% larger total accumulation bottom area than the measured. When using the D_{TA}-model obtained in this paper, the total accumulation bottom area is only 3% higher than the measured.

The results of the D_{TA}-calculation for the extended dataset, based on empirical BA-values and hypsographs, gave a mean value of 19 m and a median of 16 m. Estimation was possible for all 201 areas that had hypsographic information and values are presented in Appendix 1. The A-bottom area obtained from the wb estimates wb and wb2 and real hypsographs showed high correlation with the corresponding values calculated using Eq. 4 ($r^2 = 0.79$ and $r^2 = 0.83$). In both cases the used number of areas was n = 182 (but calculated using different wb depths). When summing the total A-bottom area calculated with Eq. 4 it was in some cases higher than the one obtained from hypsographs and in some cases lower. It is thus not possible to say if Eq. 4 over- or underestimates the calculated area.

Statistical modeling using the extended data set

By setting up linear correlation matrices it was found that BA was most correlated with Ex (r = 0.39) and At (r = 0.35), whereas D_{TA} (ln-transformed) was most

Table 6. Linear correlation between different morphometric parameters and bottom dynamic conditions (BA,%).

Parameter	Transform	r-value	Parameter	Transform	r-value
InsO (10 km)	Sqrt	0.68	ODm	^-0.9	–0.60
Awb2	ln	0.63	Ab3	ln	–0.58
Dm	ln	0.61	MFf	ln	–0.43
Dmax	ln	0.57	5p	ln	–0.39
V	ln	0.55	10p	ln	–0.38
Owb2	ln	0.54	DR	ln	–0.34
FfL	^-0.1	0.48	Ff	ln	–0.31
Au3	ln	0.46			
xm5%	–	0.45			
xm10%	Sqrt	0.43			
Ab	ln	0.39			
A	ln	0.39			
Im	^0.15	0.39			
Atot	ln	0.39			
xm	–	0.35			
W	ln	0.32			
wb	Sqrt	0.31			

Note: All values are significant at $P = 0.05$ (n = 69). Only the best variant of each parameter is presented.

correlated with DR (r = –0.77) and Dm (r = 0.49). Using SMR, the following statistical model for BA was obtained: $BA = -69.5 \cdot Ex^{0.3} - 12 \cdot \ln(DR) + 60$ ($F > 4$ in all steps). A larger exposure means a more open area which yields a deeper critical depth and smaller A-areas. A larger relative depth (DR) means a larger and shallower area, which will enable resuspension over larger areas (lower BA). DR has also previously been found to correlate well with BA in lakes.[15] The degree of explanation for the BA-model was rather low, ($r^2 = 0.31$) but on the other hand the number of analyzed areas was high, (n = 182) and the significance therefore high ($P < 0.000001$). The obtained model for D_{TA} ($r^2 = 0.65$) was: $\ln(D_{TA}) = -0.95 \cdot \ln(DR) - 5.15 \cdot Vd^{0.15} + 6.0$ with $F > 4$ in all steps. This model also includes DR and another form parameter Vd. The stability tests indicate that all model parameters are stable with low CV values (Tables 11 and 12).

Table 7. Results from first stepwise multiple regression analysis (n = 69), $F > 4$ in all steps.

Step	Equation	r^2
1	$BA = 5.3 \cdot Sqrt(InsO) + 5.9$	0.46
2	$BA = 4.3 \cdot Sqrt(InsO) + 11.6 \cdot \ln(Dm) - 15.8$	0.64
3	$BA = 4.5 \cdot Sqrt(InsO) + 18.1 \cdot \ln(Dm) - 2.5 \cdot xm - 18.3$	0.69
4	$BA = 2.9 \cdot Sqrt(InsO) + 23.5 \cdot \ln(Dm) - 3.8 \cdot xm - 7.1 \cdot \ln(5p) + 90.4$	0.74

Discussion

Empirical studies of spatial sediment distribution in coastal areas are available from many parts of the world[19,21,52,53] although not all of these relate to bottom dynamic conditions as defined here ie, focus on the fine cohesive sediment that is important for pollution. Many coupled wave, current sediment transport models have also been presented[54–57] that can be utilized to model the spatial distribution of different sediment types. These models serve many purposes, but are often difficult to use for an uninitiated user. They also often require extensive input in terms of meteorological and oceanographic forcing data, which make them less suitable for comparison of differences in the long term characteristic distribution of cohesive fine sediment (ie, bottom dynamic conditions) between many sites or coastal areas. For that type of comparison simpler models that focus on differences in morphometric characteristics and wave climate between different sites and coastal areas are preferable. Only few models with such focus have been found[27–29] and apart from the investigation by Persson and Håkanson[27] it has been difficult to find studies devoted to investigating the impact of morphometry on bottom dynamic conditions for whole coastal areas.

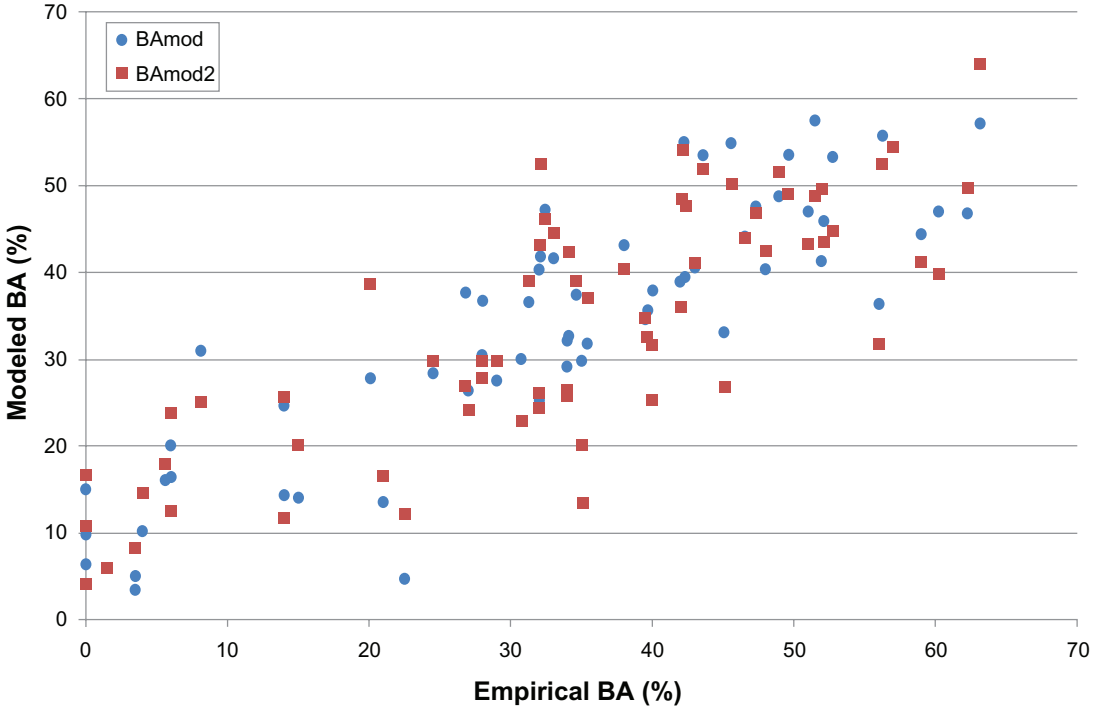

Figure 4. Modeled vs. empirical values of BA (%), n = 69.

Our results show agreement with the results by Persson and Håkanson[27] and Bekkby et al,[28] ie, that the morphometric properties of coastal areas can be used for prediction of bottom dynamic conditions. For the 69 focus areas the best statistical model yielded an r^2-value of 0.74, which is above the limits that can be considered practically useful for management purposes ($r^2 > 0.65–0.70$).[43,51] It should be pointed out that the model is only valid within the range of the investigated areas ($0.2 < InsO < 82.0\%$; $2.2 < Dm < 56.0$ m; $1.2 < xm < 13.3\%$; $3.9 \cdot 10^5 < 5p < 2.4 \cdot 10^7$ m) and should only be used outside that range with caution. Although the dataset used by Persson and Håkanson[27] was quite different from the current dataset, both Dm and xm were also included in several of their best models. The other two parameters that are included here are new parameters introduced by Lindgren[32] and were thus not available at the time of the previous investigation. The current models are based on a greater number of areas (n = 69) than the previous investigation (n = 38). Furthermore, F is above 4 in all steps and the r^2-values are considerably higher.

Table 8. Results from stability tests, 7 areas removed 10 times (n = 62, F > 4).

No	n	r^2	Model parameters and coefficients				
			Sqrt (InsO)	ln (Dm)	xm	5p	Intercept
Original	69	0.74	2.9	23.5	–3.8	–7.1	90.4
1	62	0.74	2.8	25.3	–4.7	–8.5	111.9
2	62	0.72	3.0	24.4	–4.3	–7.0	89.3
3	62	0.72	3.1	24.0	–4.2	–7.2	91.8
4	62	0.74	3.1	25.1	–4.0	–6.1	72.4
5	62	0.70	2.7	24.8	–4.3	–8.2	108.5
6	62	0.73	2.5	24.4	–4.8	–9.9	138.4
7	62	0.73	3.4	23.3	–3.9	–6.4	78.8
8	62	0.70	2.9	24.3	–4.2	–7.4	94.6
9	62	0.73	2.7	23.6	–3.7	–6.9	87.0
10	62	0.68	3.1	24.6	–4.4	–7.3	93.0
Min*	**–**	**0.68**	**2.5**	**23.3**	**–4.8**	**–9.9**	**72.4**
Mean*	**–**	**0.72**	**2.9**	**24.4**	**–4.4**	**–7.5**	**96.6**
Max*	**–**	**0.74**	**3.4**	**25.3**	**–3.7**	**–6.1**	**138.4**
CV*	**–**	**0.03**	**0.09**	**0.03**	**0.08**	**0.2**	**0.2**

Note: *The original model is not included in the statistical calculations.

The correlations and predictive power of the models must also be seen in the light of uncertainties in the empirical values of BA. For 33 of the 69 areas, mean values of BA based on two empirical values were used, but for the other 36 areas data was only available from one source. Our study of empirical BA values from different sources showed quite large differences, with an average difference of 15%-units and

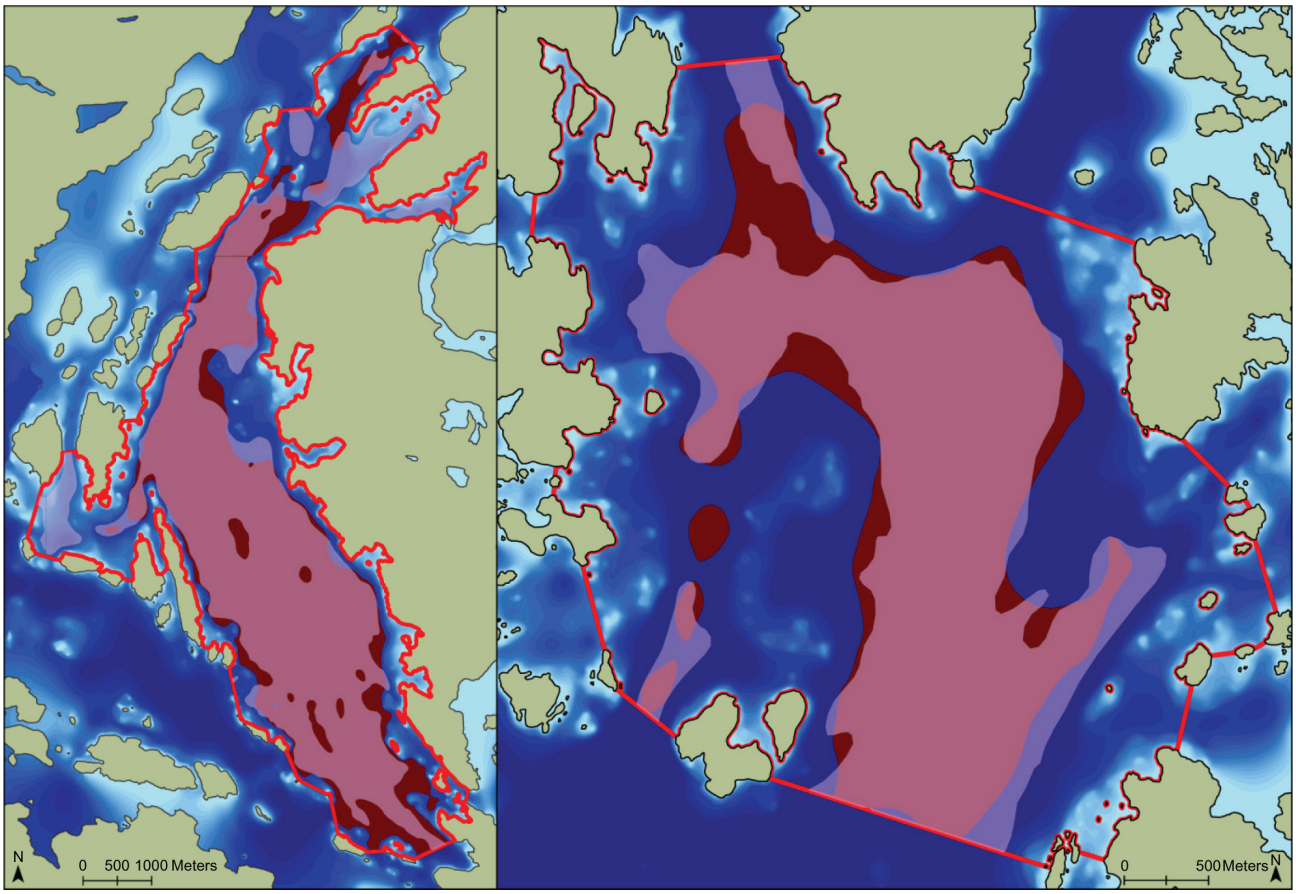

Figure 5. Maps showing measured A-areas (white) and areas under the estimated D_{TA} (red) for Östra Saxarfjärden (left) and Möja Söderfjärd (right). © Lantmäteriet Gävle 2011, Grant I 2011/0100 and © Sveriges Geologiska Undersökning.

Table 9. Morphometric parameters showing significant linear correlation ($P < 0.05$) with the ln-transformed estimated D_{TA}-value (n = 69).

Parameter	Transform	r-value	Parameter	Transform	r-value
Dm	ln	0.85	Ab3	ln	–0.81
Owb2	ln	0.82	Odm	^–0.9	–0.80
Owb	ln	0.79	DR	ln	–0.65
Dmax	ln	0.76			
xm	–	0.71			
xm5%	–	0.71			
At	ln	0.66			
wb	Sqrt	0.64			
wb2	Sqrt	0.63			
V	ln	0.61			
W	ln	0.53			
n100	ln	0.49			
E	ln	0.49			
Au3	ln	0.43			
Ff	ln	0.42			
Op	ln	0.40			
MFf	ln	0.36			
Vd	ln	0.36			
n	ln	0.36			
A	ln	0.33			

Table 10. Stability test of the D_{TA} model by removing 7 areas 10 times ($F > 4$).

Test	n	r^2	Model parameters and coefficients		
			ln(Dm)	ln(Ff)	Intercept
Original	69	0.78	0.64	0.065	0.96
1	62	0.77	0.61	0.073	1.00
2	62	0.80	0.63	0.056	1.00
3	62	0.77	0.63	0.067	0.97
4	62	0.76	0.62	0.054	1.04
5	62	0.80	0.65	0.063	0.94
6	62	0.80	0.69	0.071	0.82
7	62	0.78	0.63	0.067	0.99
8	62	0.80	0.62	0.081	0.96
9	62	0.78	0.63	0.062	0.98
10	62	0.79	0.65	0.060	0.93
Min*	**–**	**0.76**	**0.61**	**0.054**	**0.82**
Mean*	**–**	**0.79**	**0.64**	**0.065**	**0.96**
Max*	**–**	**0.80**	**0.69**	**0.081**	**1.04**
CV*	**–**	**0.02**	**0.04**	**0.13**	**0.06**

Note: The original model is not included in the statistical calculations.

a maximum difference of 54%-units. A possible reason for the observed differences could be that measurements have been carried out over different time periods. Bottom dynamic condition measurements are to some extent affected by the prevailing wind conditions in the time period preceding the measurements. This variability could lead to changes in the observed boundary between ET- and A-areas, but is unlikely to yield differences as large as those observed. Examination of the maps from the different measurements reveals that the two data sources mostly agree at the sediment sampling points; it is the areas between these points that differ in some cases. Differences in the density of investigation transects, the used swath width, navigational conditions and the complexity of bottom topography are other factors that may explain the differences in the obtained empirical determination of BA.

The BA model for the focus areas is based on four parameters. Of these the new parameter, InsO, shows the highest individual correlation with BA. InsO is quite easy to calculate and in contrast to other complex parameters like the filter factor and mean filter factor, calculation of InsO does not require any depth information. Despite its name, InsO (= Insulocity Outside) also includes a small sector inside the investigated coastal area. The size of this inside part in relation to the total depends on the size of the coastal area, the position of the center point and the direction of the circle sector. A drawback with InsO is that placement of the center point and the orientation of the circle sector is not completely objective. It is often straight

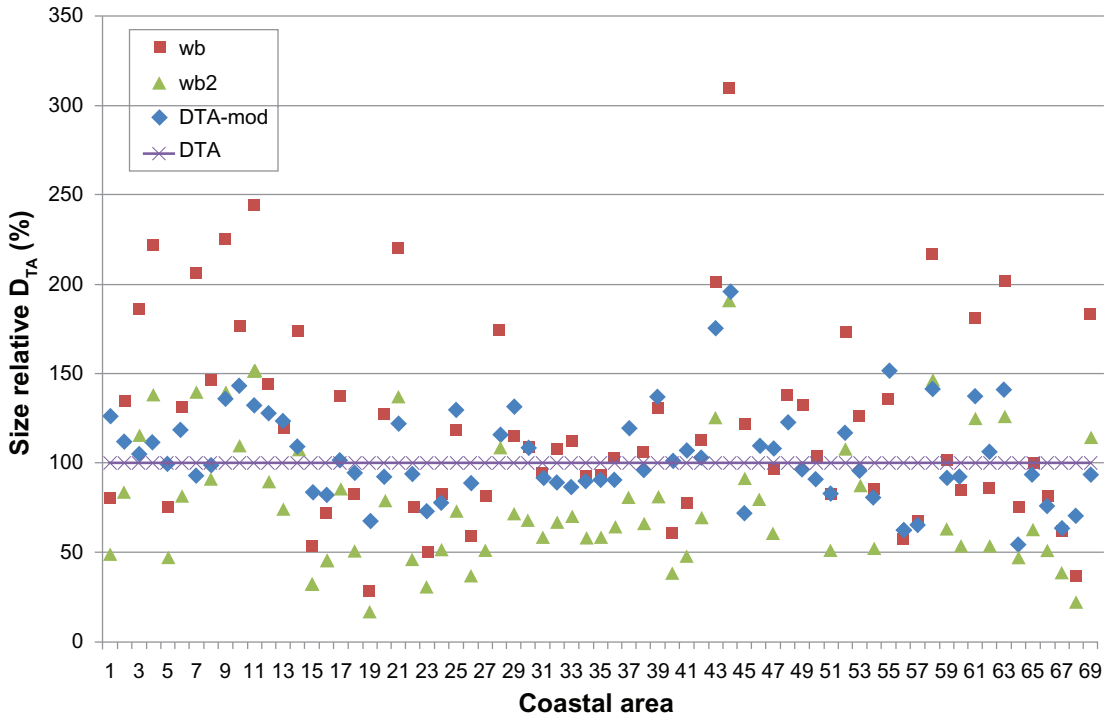

Figure 6. Size of the different wb variants in relation to the modeled and empirical estimates of the critical depth (D_{TA}).

Table 11. Stability test of the extended BA model by removing 18 areas 10 times ($F > 4$).

Test	n	r^2	Model parameters and coefficients		
			$Ex^{0.3}$	ln(DR)	Intercept
Original	182	0.31	–70	–12	60
1	164	0.32	–70	–13	60
2	164	0.31	–66	–14	56
3	164	0.31	–67	–13	59
4	164	0.30	–68	–12	60
5	164	0.29	–66	–12	58
6	164	0.28	–67	–12	59
7	164	0.30	–70	–12	61
8	164	0.29	–67	–12	59
9	164	0.34	–77	–14	63
10	164	0.31	–69	–12	60
Min*	**–**	**0.28**	**–77**	**–14**	**56**
Mean*	**–**	**0.31**	**–69**	**–13**	**59**
Max*	**–**	**0.34**	**–66**	**–12**	**63**
CV*	**–**	**0.06**	**0.05**	**0.05**	**0.03**

Note: *The original model is not included in the statistical calculations.

forward to orient the circle sector towards the sea (the direction where the most and the largest waves come from), but if the investigated area is open in many directions and lies in a region with high impact from many directions, it can be difficult. In such case a mean value can be calculated by allowing more than one sector for each area and then dividing the total

Table 12. Stability test of the extended D_{TA} model by removing 18 areas 10 times ($F > 4$).

Test	n	r^2	Model parameters and coefficients		
			ln(DR)	$Vd^{0.15}$	Intercept
Original	182	0.65	–0.95	–5.15	6.00
1	164	0.66	–1.20	–5.57	6.35
2	164	0.67	–1.19	–4.97	5.76
3	164	0.66	–1.19	–4.81	5.62
4	164	0.66	–1.20	–5.45	6.26
5	164	0.64	–1.12	–5.15	6.04
6	164	0.65	–1.15	–5.25	6.10
7	164	0.63	–1.10	–5.05	5.98
8	164	0.64	–1.11	–5.15	6.05
9	164	0.64	–1.14	–5.16	6.02
10	164	0.68	–1.22	–5.90	6.66
Min*	**–**	**0.63**	**–1.22**	**–5.90**	**5.62**
Mean*	**–**	**0.65**	**–1.16**	**–5.25**	**6.08**
Max*	**–**	**0.68**	**–1.10**	**–4.81**	**6.66**
CV*	**–**	**0.02**	**0.04**	**0.06**	**0.05**

Note: *The original model is not included in the statistical calculations.

InsO by the number of sectors used. Furthermore, the optimum radius of the sector may need further investigation. It is likely that the optimum value should be related to the size of the investigated areas. Both the investigation by Lindgren[32] and the current study showed that for the coastal area size range investigated ($0.8 < A < 13.3$ km^2 for Lindgren[32] and $0.5 < A < 46.8$ km^2 for the current investigation) a radius of 10 km shows much higher correlation with BA than a 30 km radius. Persson and Håkanson[27] observed higher correlations when separating coastal areas in direct contact with the sea from coastal areas inside an archipelago and they expressed the need to find more objective methods to make this separation. InsO is an example of a simple parameter that can possibly serve that purpose. Its inclusion may be one explanation for the good result obtained in the current study, despite not separating the two area types. Mean depth (Dm) and mean slope (xm) were other parameters that entered the best model. These parameters also previously proved to be important for bottom dynamic conditions in coastal areas[27] and lakes.[15,26] In a study from the coast outside Arendal in Norway, Bekkby et al[28] found that the distribution of soft sediment (similar to A-bottom areas) was primarily dependent on depth, terrain curvature and (modeled) current speed at the seafloor and that the prediction was only slightly better when including current speed. They also included the slope at each specific point in their investigation, but this parameter did not feature in the best model. In another study by Bekkby et al,[29] slope was identified as the single most important factor for identification of a rocky seabed. Slope calculations are dependent on the resolution of the bathymetric model, where a courser resolution generally gives a lower slope.[58] This was tested and for the investigated areas a doubled raster resolution was found to increase the mean slope by only about 1%-unit. Several studies have shown that different algorithms for slope calculation perform differently and that these differences can be quite large.[58–60] All slope calculations in the current investigation were performed using the 3D-analyst extension in ArcGIS 9.3 and according to Jones[60] that type of algorithm, which uses a 3×3 neighborhood, performs well. The partial internal correlation between mean slope and Dm (although $r < 0.75$), is likely to be the reason for the change in sign that can be noted for xm from Table 6 to Table 7. A change of

sign like this may at first seem illogical and look like a possible error. However in multiple regression the sign of a parameter may depend on other terms in the model and a change of sign does not mean that the regression is wrong.[39–41] Although xm shows positive individual correlation with BA, much of that correlation is due to the correlation between xm and Dm and the simultaneous high correlation between Dm and BA. In multiple regression the effects from these two parameters on BA are partially separated and then xm has a negative effect on BA, which was also the result in several other studies.[27,29,61] The logical explanation for this may be the occurrence of slope induced ET-areas. A changed sign may be an indicator of error introduced by multicollinearity if *P*-values are large and the coefficients are close to zero. In this case all *P*-values are very small and the coefficients are far from zero. Also, the internal correlation between the two parameters is not very high and F is far above 4. So in this case the changed sign does not likely indicate error in the regression, but causes some difficulty in interpreting the causal relationship between mean slope and BA. Because of this, the role of slope in relation to bottom dynamic conditions needs to be investigated further.

The focus of the current paper is the influence of morphometry on bottom dynamic conditions and there are many other factors affecting bottom dynamic conditions that have not been accounted for here. Submerged plants (macrophytes) lower current velocities and thus generally increase sedimentation and decrease resuspension.[62] If detailed data on Secchi depth were available the extent of submerged plants could be estimated and included in the analysis. Benthic animals (zoobenthos) and microbes also affect sediment stability and thus transport and erosion.[63] The sediment can, eg, be stabilized by secretes from benthic microbes and the grain size can be altered.[64–66] With access to spatial data on deep water oxygen concentrations the absence of zoobenthos could also be included in a GIS-analysis. When river action is large enough it can affect bottom dynamic conditions because currents from the river (and corresponding compensation currents) can cause resuspension, even below the critical depth. Several areas in the SGU dataset, and some in the focus dataset, are affected by river action. When studying the bottom dynamic maps from the two focus areas influenced by the largest rivers: River Norrström with a mean discharge of 175 m^3 s^{-1} into Saltsjön[47] and River Ångermanälven with a mean discharge of 450 m^3 s^{-1} into Ångermanfjorden[47] it is clear that the influence from river action is small. Increased salinity also increases the resistance to erosion of cohesive sediment.[67,68] All but three of the focus areas lie in the brackish Baltic Sea where the salinity ranges from approximately 2 to 8 and the salinity differences between these areas are hence small. The larger difference in salinity between the Swedish west coast (salinities ranging between approx 15–30)[36] and the Baltic Sea may possibly be of some importance. Turbulence caused by ships (propeller wash) is another factor that can cause sediment erosion below the critical depth and thus affects bottom dynamic conditions.[69] Although this effect is local and only noticeable down to a certain depth, some of the areas in the focus dataset (Saltsjön, Norra Lilla Värtan and Södra Lilla Värtan) are located close to central Stockholm and the passage of large ships is frequent through these areas. Saltsjön and Södra Lilla Värtan have empirical estimates of the critical depth at 18–19 m and Norra Lilla Värtan has an empirical D_{TA} estimate of 12 m. In a study of Oslo harbor in Norway, Lepland et al[69] found effects from propeller wash on the sediment down to depths between 21–23 m, so there may be a noticeable effect of propeller wash in Saltsjön and Lilla Värtan. In Norra Lilla Värtan this effect may even be quite large locally. To assess whether this influence is large enough to affect the BA-values used and the analysis, the spatial extent of areas affected by ships must be studied. However, no such data were available, so estimation of the possible influence of propeller wash was not possible. Wind direction, speed and duration have great effect on waves and hence also on bottom dynamic conditions. Furthermore it has been demonstrated that it is important to include meteorological conditions when predicting bottom dynamic conditions for large sea basins.[30] In coastal areas morphometry is more important because there a more complex morphometry and frequent occurrence of islands restrict the fetch. Prevailing wind directions could be of special importance in coastal areas which have boundaries with adjacent areas in only one direction. To account for this Lindgren[32] modified the filter factor, but did not obtain any improved correlation with BA. Inclusion of wind could possibly

increase correlation with BA, but it is not obvious how to best incorporate effects from wind together with morphometric properties in a statistical model. The morphometric parameters than have been used in this study can easily be calculated from maps and sea charts using geographic information systems. Inclusion of typical wind conditions for each area would require site specific wind data which may not be as easily obtained as the morphometric parameters and interpolation would likely be necessary. The investigated areas are non-tidal or have only low tidal amplitudes and morphometry should be an essential factor affecting bottom dynamic conditions in most non-tidal coastal areas. In areas highly affected by tides bottom dynamic conditions are strongly affected by tidal currents[70–72] and morphometry thus plays a different role.

The model for estimating the critical depth should be seen as an alternative way to obtain a value of BA. The empirical D_{TA} estimates that were used to develop the model were calculated from empirical BA-values and hypsographs. GIS-analysis showed that for many coastal areas the areas under D_{TA} and empirically identified A-areas coincide well. However, the calculation of D_{TA} was made possible by assuming that the deepest bottom areas are always only A-areas and in reality there may also be ET-areas in deep bottom areas (due to steep slopes and currents) and A-areas in more shallow bottom areas (eg, in sheltered embayments), see conceptual sketch in Figure 7. For one specific area a lower wave base (higher D_{TA}-value) means more ET-areas and less A-areas, but when comparing many areas the relationship between the wave base and the depth distribution of each area, ie, the bathymetry, determines the proportion of the bottom being affected by waves and hence functioning as ET-bottom areas. A wave base of 10 m in a shallow coastal area like Fabriksviken (Dm ≈ 2.5 m, Dmax ≈ 7 m) means the area consists almost solely of ET-areas with a very small proportion of A-areas. The same wave base of 10 m will have little effect on the bottom dynamic conditions in a deep area like Östra Saxarfjärden (Dm ≈ 30 m, Dmax ≈ 68 m). This illustrates the importance of accounting both for factors describing wave influence (like exposure and sheltering effects from islands) and factors relating to the effect waves have on the sediment (like depth and slope).

The statistical models developed in this paper are based on samples of coastal areas from the Swedish coast and are hence, strictly, only valid for those areas. If the models are used in other areas, each included variable should be within the range that was used to obtain the model. The 69 areas in the smaller dataset include a wide morphometric range (of, eg, size, depth and openness) which many other Swedish coastal areas fall within. Although the extended dataset may seem relatively regionally focused (Fig. 1), it includes nearly one third of all Swedish coastal areas (based on SMHI[46,47]). Many other coastal areas in the Baltic Sea, should fall within the wide morphometric range present in that dataset. The purpose of the investigation was to study general patterns in bottom dynamic conditions, the critical depth and factors affecting these two parameters. The statistical analysis performed in this paper hopefully has contributed to clarifying such general patterns, and some causal relationships have been explored and discussed that may also be valid elsewhere.

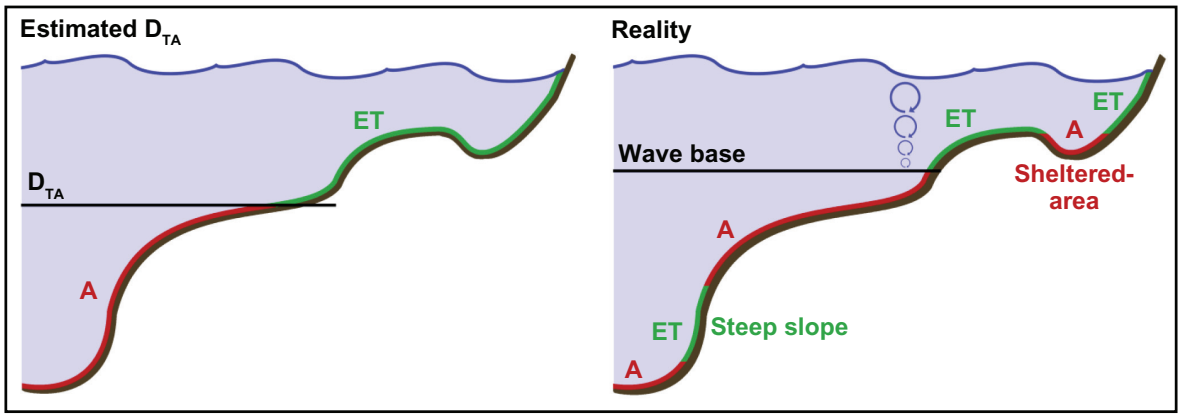

Figure 7. Conceptual sketch illustrating some principal differences between the estimated D_{TA} and reality.

Conclusions

Using data from Swedish coastal areas statistical models have been developed for prediction of bottom dynamic conditions and critical depth solely based on morphometric parameters. The best statistical model of the proportion of A-bottom areas (BA, %) yielded an r^2-value of 0.74. Significant correlation was found between many morphometric properties of coastal areas and bottom dynamic conditions. The proportion of sheltering islands outside the investigated area had the highest individual correlation with BA ($r = 0.68$). Mean depth (Dm) and mean slope (xm) were also important for bottom dynamic conditions among the investigated coastal areas. Classification of steep slopes using two static limits (5% and 10%) was tested, but although this gave better simple linear correlation with BA, mean slope still entered the best multiple regression model instead.

A comparison of empirical data on the proportion of accumulation areas from two independent sources covering 33 areas showed large differences for many areas with an average difference of 15 percentage units and a maximum difference of 54 percentage units. The linear correlation between the two empirical datasets was only $r^2 = 0.22$. This suggests that the uncertainty in empirical bottom dynamic condition data is high.

New values of the proportion of accumulation areas (BA) have been presented for 209 Swedish coastal areas with a mean value of 27%. For 201 of these areas hypsographs were available, which enabled estimation of the critical depth (D_{TA}) as well. The mean value of D_{TA} among these 201 areas was 19 m.

Disclosures

This manuscript has been read and approved by all authors. This paper is unique and not under consideration by any other publication and has not been published elsewhere. The authors and peer reviewers report no conflicts of interest. The authors confirm that they have permission to reproduce any copyrighted material.

Acknowledgements

The authors thank Professor Lars Håkanson, Swedish University of Agricultural Sciences and Dr. Andreas Bryhn, Uppsala University, for giving valuable comments on this paper. Emma Henningsson at Excellent English is thanked for English copyediting. Furthermore the Geological Survey of Sweden (SGU) is acknowledged for the kind free provision of marine geological maps (© Sveriges Geologiska Undersökning, SGU) that were used in this study.

References

1. Jarre-Teichmann A. The potential role of mass balance models for the management of upwelling ecosystems. *Ecological Applications*. 1998;8 Suppl: S93–103.
2. Vidal M, Duarte CM, Sánchez MC. Coastal eutrophication research in Europe: progress and imbalances. *Marine Pollution Bulletin*. 1999;38:851–4.
3. Kawamoto K, MacLeod M, Mackay D. Evaluation and comparison of multimedia mass balance models of chemical fate: application of EUSES and ChemCAN to 68 chemicals in Japan. *Chemosphere*. 2001;44:599–612.
4. Giblin AE, Vallino JJ. The role of models in addressing coastal eutrophication. In: Canham CD, Cole JJ, Laurenroth WK, editors. *Models in Ecosystem Science*. New Jersey: Princeton University Press; 2003:327–43.
5. Nobre AM, Ferreira JG, Nunes JP, et al. Assessment of coastal management options by means of multilayered ecosystem models. *Estuarine, Coastal and Shelf Science*. 2010;87:43–62.
6. Förstner U, Wittmann GTW. *Metal Pollution in the Aquatic Eenvironment*. Berlin: Springer-Verlag; 1981.
7. Wu S, Gschwend PM. Sorption kinetics of hydrophobic organic compounds to natural sediments and soils. *Environmental Science and Technology*. 1986;20:717–25.
8. Sly PG, Hart BT, editors. Sediments and Water Interactions: Proceedings of the Third International Symposium on Interactions Between Sediments. Berlin: Springer-Verlag; 1986.
9. Mackay D. *Multimedia Environmental Models: The Fugacity Approach*. 2nd ed. Boca Raton: CRC Press, Taylor & Francis Group; 2001.
10. Håkanson L. Suspended Particulate Matter in Lakes, Rivers, and Marine Systems. New Jersey: The Blackburn Press; 2005.
11. Malmaeus JM, Eklund J, Karlsson OM, Lindgren D. The optimal size of dynamic phosphorus models for Baltic coastal areas. *Ecological Modelling*. 2008;216:303–15.
12. Karlsson OM, Malmaeus JM, Josefsson S, Wiberg K, Håkanson L. Application of a mass-balance model to predict PCDD/F turnover in a Baltic coastal estuary. *Estuarine, Coastal and Shelf Science*. 2010;88:209–18.
13. Sly PG. Sedimentary processes in lakes. In: Lerman A, editor. *Lakes: Chemistry, Geology, Physics*. Berlin-Heidelberg-New York: Springer Verlag; 1978:65–89.
14. World Meteorological Organization. *Guide to Wave Analysis and Forecasting*. Geneva: Secretariat of the World Meteorological Organization; 1998. WMO-No. 702.
15. Håkanson L, Jansson M. *Principles of Lake Sedimentology*. Berlin: Springer-Verlag; 1983.
16. Kiirikki M. Mechanisms affecting macroalgal zonation in the northern Baltic Sea. *European Journal of Phycology*. 1996;31:225–32.
17. Koch EW. Beyond light: physical, geological, and geochemical parameters as possible submersed aquatic vegetation habitat requirements. *Estuaries*. 2001;24:1–17.
18. Stål J, Paulsen S, Pihl L, Rönnbäck P, Söderqvist T, Wennhage H. Coastal habitat support to fish and fisheries in Sweden: Integrating ecosystem functions into fisheries management. *Ocean and Coastal Management*. 2008;51:594–600.
19. Wright LD, Prior DB, Hobbs CH, et al. Spatial variability of bottom types in the lower Chesapeake Bay and adjoining estuaries and inner shelf. *Estuarine, Coastal and Shelf Science*. 1987;24:765–84.
20. Kenny AJ, Andrulewicz E, Bokuniewicz H, et al. *An overview of seabed mapping technologies in the context of marine habitat classification*. Copenhagen: International Council for the Exploration of the Sea, ICES; 2000; C.M.2000/T:10.
21. Jonsson P, Persson J, Holmberg P. *Skärgårdens bottnar*. Stockholm: National Swedish Environmental Protection Agency (SNV); 2003. Report No. 5212.

22. Sutton G, Boyd S, editors. *Effects of extraction of marine sediments on the marine environment 1998–2004*. Copenhagen: International Council for the Exploration of the Sea; 2009. ICES Cooperative Research Report No. 297.
23. Håkanson L, Rosenberg R. *Praktisk kustekologi*. Solna: National Swedish Environmental Protection Agency (SNV); 1985. Report No. 1987.
24. Håkanson L, Eklund JM. A dynamic mass balance model for phosphorus fluxes and concentrations in coastal areas. *Ecological Research*. 2007;22: 296–320.
25. Stanley DJ, Swift DJP, editors. *Marine Sediment Transport and Environmental Management*. New York: John Wiley & Sons; 1976.
26. Rowan DJ, Kalff J, Rasmussen JB. Estimating the mud deposition boundary depth in lakes from wave theory. *Canadian Journal of Fisheries and Aquatic Sciences*. 1992;49:2490–7.
27. Persson J, Håkanson L. Prediction of bottom dynamic conditions in coastal waters. *Marine and Freshwater Research*. 1995;46:359–71.
28. Bekkby T, Nilsson HC, Olsgard F, Rygg B, Isachsen PE, Isaeus M. Identifying soft sediments at sea using GIS-modelled predictor variables and sediment profile image (SPI) measured response variables. *Estuarine, Coastal and Shelf Science*. 2008;79:631–6.
29. Bekkby T, Moy FE, Kroglund T, et al. Identifying rocky seabed using GIS-modeled predictor variables. *Marine Geodesy*. 2009;32:379–90.
30. Brydsten L. Characterization of transport bottoms in the Gulf of Bothnia—a model approach. *Aqua Fennica*. 1993;23:153–64.
31. Jönsson A, Danielsson Å, Rahm L. Bottom type distribution based on wave friction velocity in the Baltic Sea. *Continental Shelf Research*. 2005;25: 419–35.
32. Lindgren D. Determining openness and energy filtering in coastal areas using geographic information systems. *Estuarine, Coastal and Shelf Science*. 2011;91:177–86.
33. Persson J, Håkanson L, Wallin M. Ett geografiskt informations system för kustvatten—planering baserat på sjökorts information. Copenhagen: Nordic Council of Ministers; 1994. TemaNord 1994:667. (in Swedish with English summary).
34. Håkanson L, Kulinski I, Kvarnäs H. *Vattendynamik och bottendynamik i kustzonen*. Solna: National Swedish Environmental Protection Agency (SNV); 1984. SNV PM 1905.
35. Pilesjö P, Persson J, Håkanson L. Digital bathymetric information for calculations of morphometrical parameters and surface water retention time for coastal areas (in Swedish). Solna: National Swedish Environmental Protection Agency (SNV); 1991. Report No. 3916.
36. Lindgren D, Håkanson L. Morphometric classification and GIS-based data analysis in coastal modeling and management. *Open Environmental Sciences*. 2011;5:1–17.
37. Wessel P, Smith WHF. A global, self-consistent, hierarchical, high-resolution shoreline database. *Journal of Geophysical Research*. 1996; 101:8741–3.
38. Wallin M, Håkanson L, Persson J. *Nutrient loading models for coastal waters- especially for the assessment of environmental effects of marine fish farms*. Copenhagen: Nordic Council of Ministers; 1992. Nordiske Seminar- og Arbejdsrapporter; 1992:502.
39. Ryan TP. *Modern Regression Methods*. New York: John Wiley & Sons; 1997.
40. Ryan TP. *Modern Engineering Statistics*. New Jersey: John Wiley & Sons; 2007.
41. Weisberg S. *Applied Linear Regression*. 3rd ed. New Jersey: John Wiley & Sons; 2005.
42. Rubin A. *Statistics for Evidence-based Practice and Evaluation.* Belmont: Brooks/Cole; 2009.
43. Håkanson L, Peters RH. *Predictive Limnology—Methods for predictive modelling*. Amsterdam: SPB Academic Publishers; 1995.
44. Osborne JW. Improving your data transformations: Applying the Box-Cox transformation. *Practical Assessment, Research and Evaluation*. 2010;15: No 12.
45. Montgomery DC, Peck EA, Vining GG. *Introduction to Linear Regression Analysis*. 3rd ed. New York: Wiley; 2001.
46. SMHI. *Havsområdesregister 1993*. Norrköping: Swedish Meteorological and Hydrological Institute (SMHI); 1994. Oceanografi No. 60.
47. SMHI. *Djupdata för havsområden 2003*. Norrköping: Swedish Meteorological and Hydrological Institute (SMHI); 2003. Oceanografi No. 73.
48. SMHI. *Djupdata för havsområden 2003, Uppdateringar 2004*. [Database]. Available at: http://www.smhi.se/sgn0102/n0205/havsomr/havsomr2004.zip. Accessed April 6 2010.
49. Håkanson L. *Lakes—Form and Function*. Caldwell, New Jersey: The Blackburn Press; 2004.
50. Lindgren D. Assessment of ecological value of coastal areas using morphometry and Secchi depth: a case study with data from the Swedish coast. *Journal of Coastal Research*. 2010;26:429–35.
51. Prairie, YT. Evaluating the predictive power of regression models. *Canadian Journal of Fisheries and Aquatic Sciences*. 1996;53:490–2.
52. Lee HJ, Chough SK. Sediment distribution, dispersal and budget in the yellow sea. *Marine Geology*. 1989;87:195–205.
53. Persson J, Jonsson P. Historical development of laminated sediments—an approach to detect soft sediment ecosystem changes in the Baltic Sea. *Marine Pollution Bulletin*. 2000;40:122–34.
54. Lumborg U, Windelin A. Hydrography and cohesive sediment modelling: application to the Rømø Dyb tidal area. *Journal of Marine Systems*. 2003;38: 287–303.
55. Warner JC, Sherwood CR, Signell RP, Harris CK, Arango HG. Development of a three-dimensional, regional, coupled wave, current, and sediment-transport model. *Computers and Geosciences*. 2008;34:1284–306.
56. Bakhtyar R, Ghaheri A, Yeganeh-Bakhtiary A, Barry DA. Process-based model for nearshore hydrodynamics, sediment transport and morphological evolution in the surf and swash zones. *Applied Ocean Research*. 2009;31: 44–56.
57. Idier D, Romieu E, Pedreros R, Oliveros C. A simple method to analyse non-cohesive sediment mobility in coastal environment. *Continental Shelf Research*. 2010;30:365–77.
58. Warren SD, Hohmann MG, Auerswald K, Mitasova H. An evaluation of methods to determine slope using digital elevation data. *Catena*. 2004;58:215–33.
59. Srinivasan R, Engel BA. Effect of slope prediction methods on slope and erosion estimates. *Applied Engineering in Agriculture*. 1991;7:779–83.
60. Jones KH. A comparison of algorithms used to compute hill slope as a property of the DEM. *Computers and Geosciences*. 1998;24:315–23.
61. Blais JM, Kalff J. The influence of lake morphometry on sediment focusing. *Limnology and Oceanography*. 1995;40:582–8.
62. Madsen JD, Chambers PA, James WF, Koch EW, Westlake DF. The interaction between water movement, sediment dynamics and submersed macrophytes. *Hydrobiologica*. 2001;444:71–84.
63. Le Hir P, Monbet Y, Orvain F. Sediment erodability in sediment transport modelling: can we account for biota effects? *Continental Shelf Research*. 2007;27:1116–42.
64. Jumars PA, Nowell ARM. Effects on benthos on sediment transport: difficulties with functional grouping. *Contintental Shelf Research*. 1984;3:115–30.
65. Lelieveld SD, Pilditch CA, Green MO. Variation in sediment stability and relation to indicators of microbial abundance in the Okura Estuary, New Zealand. *Estuarine, Coastal and Shelf Science*. 2003;57:123–36.
66. Stal LJ. Microphytobenthos as a biogeomorphological force in intertidal sediment stabilization. *Ecological Engineering*. 2010;36:236–45.
67. Gularte RC, Kelly WE, Nacci VA. Erosion of cohesive sediments as a rate process. *Ocean Engineering*. 1980;7:539–51.
68. Dyer KR. *Coastal and Estuarine Sediment Dynamics*. New York: John Wiley & Sons; 1986.
69. Lepland A, Andersen TJ, Lepland A, et al. Sedimentation and chronology of heavy metal pollution in Oslo harbor, Norway. *Marine Pollution Bulletin*. 2010;60:1512–22.
70. Masselink G, Pattiaratchi C. Tidal asymmetry in sediment resuspension on a macrotidal beach in northwestern Australia. *Marine Geology*. 2000;163: 257–74.
71. Manning AJ, Langston WJ, Jonas PJC. A review of sediment dynamics in the Severn Estuary: influence of flocculation. *Marine Pollution Bulletin*. 2010;61:37–51.
72. Shi JZ. Tidal resuspension and transport processes of fine sediment within the river plume in the partially-mixed Changjiang River estuary, China: A personal perspective. *Geomorphology*. 2010;121:133–51.

Supplementary Data

Appendix A

Proportion of accumulation bottom areas (BA, %) and estimated critical depth (D_{TA}, m) for 209 Swedish coastal areas calculated using maps from SGU (© Sveriges geologiska undersökning) and boundaries, areas and hypsographs from SMHI.[47,48] Cover (%) describes the proportion of the area that was covered by the SGU-map data. Where values of D_{TA} are missing, depth data are missing in the Swedish Sea Registry.[47,48]

HID	Name	Basin	Cover (%)	BA (%)	Estimated D_{TA} (m)
SE634230-201605	Västerfjärden	Bothnian Sea	94.3	0	10.0
SE634200-202033	Österfjärden	Bothnian Sea	97.3	2.9	16.1
SE633870-202230	Fjärdgrundsområdet sek namn	Bothnian Sea	98.5	0	25.0
SE633710-200500	Mjölefjärden	Bothnian Sea	99.6	0	35.0
SE633460-195860	Hörnefors området sek namn	Bothnian Sea	99.4	0	27.0
SE633000-195000	Örefjärden	Bothnian Sea	98.3	3.2	22.1
SE625900-174360	Bollstafjärden	Bothnian Sea	96.6	44.8	21.4
SE625500-175153	Kramforsfjärden sek namn	Bothnian Sea	85.8	53.9	18.3
SE625180-181655	Gaviksfjärden	Bothnian Sea	97.5	6.3	77.1
SE624870-175500	Ramöfjärden sek namn	Bothnian Sea	98.5	25.7	39.4
SE624800-181030	Grönsviksfjärden	Bothnian Sea	98.0	0	64.0
SE624615-180500	Storfjärden	Bothnian Sea	97.2	25.7	70.0
SE624335-180000	Hemsösundet sek namn	Bothnian Sea	73.1	2.2	–
SE623980-175600	Älandsfjärden	Bothnian Sea	79.2	0	–
SE623810-180350	Norra sundet	Bothnian Sea	63.2	0	–
SE622860-173000	Klingerfjärden	Bothnian Sea	83.9	30.8	18.4
SE622500-172430	Alnösundet	Bothnian Sea	97.1	34.0	15.9
SE622339-172190	Sundsvallsfjärden	Bothnian Sea	95.2	36.1	13.9
SE622126-172430	Draget	Bothnian Sea	98.5	33.0	27.5
SE622000-172300	Svartviksfjärden	Bothnian Sea	82.7	42.7	15.6
SE621855-174000	Sundsvallsbukten	Bothnian Sea	98.9	6.7	83.6
SE604250-173000	Skutskärsfjärden sek namn	Bothnian Sea	97.8	4.5	33.4
SE604200-171765	Yttre Fjärden	Bothnian Sea	91.3	37.9	10.1
SE595000-185600	Vätösundet	Bothnian Sea	91.8	49.2	10.1
SE594800-190655	N Lidöfjärden sek namn	Bothnian Sea	61.3	15.8	–
SE594800-190220	Björköfjärden	Bothnian Sea	85.8	44.8	10.4
SE594845-191240	Havssvalget	Baltic Proper	98.9	7.6	38.1
SE594670-185500	Norrtäljeviken	Baltic Proper	89.7	33.6	10.1
SE594590-190600	Tjocköfjärden	Baltic Proper	93.9	7.1	28.9
SE594384-185542	Åkeröfjärden	Baltic Proper	68.4	45.3	–
SE594275-191000	Granhamnsfjärden	Baltic Proper	97.0	6.4	41.1
SE594260-185580	Längfjärden	Baltic Proper	77.0	9.7	–
SE594100-185690	Ålandsfjärden sek namn	Baltic Proper	95.1	19.5	15.4
SE594000-190500	Gräsköfjärden	Baltic Proper	99.2	9.1	23.9
SE593920-191440	Vidingefjärden	Baltic Proper	99.0	13.4	27.5
SE593860-192000	Nätfjärden	Baltic Proper	96.0	0	41.0
SE593820-185500	Blidösund	Baltic Proper	97.4	13.8	16.0
SE593750-184900	Yxlaområdet	Baltic Proper	96.7	38.3	10.9
SE593750-183962	Bergshamraviken	Baltic Proper	95.7	33.5	4.0
SE593500-191660	Nö Kobbfjärden sek namn	Baltic Proper	98.9	7.7	37.3
SE593500-190000	Svartlögafjärden	Baltic Proper	98.8	4.8	30.2
SE593460-184890	Skatfjärden	Baltic Proper	97.6	36.8	6.9

(*Continued*)

(*Continued*)

HID	Name	Basin	Cover (%)	BA (%)	Estimated D_{TA} (m)
SE593300-183600	Norrfjärden sek namn	Baltic Proper	98.0	29.6	16.7
SE593180-191280	Kobbfjärden	Baltic Proper	99.5	21.0	47.5
SE593080-184500	Gälnan	Baltic Proper	98.5	29.7	8.9
SE593000-192000	Ormskärsfjärden sek namn	Baltic Proper	91.8	6.1	42.7
SE593000-190500	Kallskärsfjärden	Baltic Proper	98.9	14.2	42.0
SE592790-183000	Östra Saxarfjärden	Baltic Proper	99.1	52.5	22.4
SE592650-182815	Västra Saxarfjärden	Baltic Proper	99.0	40	20.7
SE592640-184500	Träsköfjärden	Baltic Proper	96.9	22.9	7.0
SE592605-182310	Trälhavet	Baltic Proper	98.7	42.4	20.2
SE592600-181600	Säbyvik	Baltic Proper	94.7	52.4	7.8
SE592600-181135	Kyrkfjärden	Baltic Proper	97.5	88.4	1.9
SE592575-181770	Överbyfjärden	Baltic Proper	96.2	47.6	9.0
SE592547-182720	Lindalssundet	Baltic Proper	96.8	25.1	20.6
SE592515-182020	Kodjupet	Baltic Proper	95.9	52.8	5.1
SE592500-185000	Möja västerfjärd	Baltic Proper	98.2	33.1	42.8
SE592468-182000	Norra Vaxholmsfjärden	Baltic Proper	98.1	39.7	10.8
SE592435-182400	Rindösundet	Baltic Proper	98.8	42.3	8.8
SE592420-182210	Södra Vaxholmsfjärden	Baltic Proper	97.0	34.8	15.3
SE592400-184400	Skagsfjärden	Baltic Proper	95.6	6.6	15.5
SE592400-181860	Tallaröfjärden	Baltic Proper	92.8	60.4	5.0
SE592400-180800	Stora Värtan	Baltic Proper	98.7	63.3	6.9
SE592315-182620	Solöfjärden	Baltic Proper	95.3	23.7	24.3
SE592290-181600	Askrikefjärden	Baltic Proper	98.9	32.4	21.8
SE592280-183550	Sandöfjärden	Baltic Proper	98.7	28.7	24.2
SE592245-184400	Sollenkrokafjärden	Baltic Proper	97.2	0	61.0
SE592200-180625	Tranholmenområdet sek namn	Baltic Proper	97.2	74.5	6.4
SE592135-182700	Torsbyfjärden	Baltic Proper	99.0	45.7	20.3
SE592090-185125	Möja söderfjärd	Baltic Proper	95.7	23.1	54.5
SE592040-184000	Älgöfjärden	Baltic Proper	95.4	14.0	17.4
SE592000-190500	Björkskärsfjärden	Baltic Proper	98.8	3.1	45.9
SE592000-184700	Kanholmsfjärden	Baltic Proper	99.0	54.4	51.6
SE592000-181015	Lilla Värtan	Baltic Proper	99.2	57.4	17.6
SE591920-180800	Strömmen	Baltic Proper	96.4	57.3	8.9
SE591910-185600	Rödkobbsfjärden	Baltic Proper	98.5	23.0	20.5
SE591905-185275	Eknösundet	Baltic Proper	97.9	9.3	51.2
SE591815-182670	Grisslingen	Baltic Proper	96.4	54.6	10.0
SE591800-181360	Skurusundet	Baltic Proper	95.5	48.8	10.4
SE591790-185500	Getholmsfjärden sek namn	Baltic Proper	95.5	0	44.0
SE591760-181955	Baggensfjärden	Baltic Proper	99.2	43.5	20.6
SE591755-183895	Breviken	Baltic Proper	95.5	7.9	24.4
SE591755-182800	Lagnöström	Baltic Proper	95.1	52.6	4.1
SE591745-182250	Kolström	Baltic Proper	78.9	56.7	–
SE591655-183200	Tranaröfjärden	Baltic Proper	93.6	30.3	10.5
SE591500-185300	Brandfjärden	Baltic Proper	97.7	11.2	10.2
SE591400-182320	Erstaviken	Baltic Proper	99.4	45.3	23.7
SE591330-184225	Kalkkobbsfjärden	Baltic Proper	98.3	19.2	29.1
SE591300-182800	Ingaröfjärden	Baltic Proper	99.1	31.3	27.3
SE591280-182070	Kalvfjärden	Baltic Proper	93.8	71.2	3.8
SE591200-183600	Nämdöfjärden	Baltic Proper	98.7	29.6	52.6
SE591175-185000	Bulleröfjärden	Baltic Proper	97.3	10.6	6.0
SE591160-182400	Ällmorafjärden	Baltic Proper	98.0	24.0	12.1
SE591090-182300	Vissvassfjärden	Baltic Proper	94.6	50.2	8.2
SE591050-182740	Gränöfjärden	Baltic Proper	96.9	13.7	27.0
SE591050-182320	Åvaviken	Baltic Proper	98.9	46.4	10.4

(*Continued*)

(*Continued*)

HID	Name	Basin	Cover (%)	BA (%)	Estimated D_{TA} (m)
SE590835-183000	Jungfrufjärden	Baltic Proper	99.2	39.6	48.5
SE590730-183763	Norrfjärden	Baltic Proper	97.2	17.7	16.2
SE590700-174145	Hallsfjärden	Baltic Proper	93.6	28.6	15.6
SE590665-184210	Biskopsfjärden	Baltic Proper	95.7	8.0	6.6
SE590635-182120	Sandemars fjärd sek namn	Baltic Proper	97.2	21.3	13.8
SE590550-174540	Kaggfjärden	Baltic Proper	96.1	78.6	9.0
SE590500-182000	Fäglaröfjärden sek namn	Baltic Proper	96.7	7.9	33.7
SE590400-174090	Näslandsfjärden	Baltic Proper	93.6	51.0	10.0
SE590385-180890	Horsfjärden	Baltic Proper	95.6	60.2	5.0
SE590200-173765	Stavbofjärden	Baltic Proper	91.1	69.6	3.1
SE590148-183625	Norstensfjärden	Baltic Proper	98.6	9.1	34.8
SE590000-183000	Hanstensfjärden	Baltic Proper	97.2	13.4	41.7
SE590000-174400	Himmerfjärden	Baltic Proper	98.7	64.9	13.1
SE585500-180500	Mysingen	Baltic Proper	98.5	31.5	29.4
SE585400-173870	Gälöfjärden	Baltic Proper	95.5	62.5	5.7
SE585345-174950	Fällnäsviken	Baltic Proper	94.4	92.1	1.0
SE585200-174000	Fifängsdjupet	Baltic Proper	98.4	41.8	14.6
SE585200-173600	Fägelöfjärden	Baltic Proper	95.1	69.7	3.6
SE585200-173430	Trosafjärden	Baltic Proper	87.1	41.0	2.6
SE585170-175445	Nynäsviken	Baltic Proper	94.6	87.6	2.9
SE585145-175690	Gärdsfjärden	Baltic Proper	97.4	0	34.0
SE585075-173130	Hällsviken	Baltic Proper	95.8	11.3	18.0
SE585040-173535	Gillsviken	Baltic Proper	94.8	31.2	6.3
SE585000-174600	Svärdsfjärden	Baltic Proper	98.2	50.9	15.8
SE584960-175280	Dragfjärden sek namn	Baltic Proper	91.1	78.1	3.0
SE584905-172980	Skettnefjärden	Baltic Proper	94.7	15.3	12.5
SE584870-174310	Asköfjärden	Baltic Proper	98.5	22.0	22.0
SE584840-175400	Konabbsfjärden	Baltic Proper	97.7	0	50.0
SE584820-172920	Gunnarbofjärden	Baltic Proper	92.3	9.9	13.4
SE584695-175315	S Konabbsfjärden sek namn	Baltic Proper	98.2	0	35.0
SE584600-173200	Gupafjärden	Baltic Proper	97.0	19.9	20.7
SE584520-172495	Tvären	Baltic Proper	97.4	42.8	16.2
SE584435-170450	Mellanfjärden	Baltic Proper	90.2	59.4	1.9
SE584434-170260	Stadsfjärden	Baltic Proper	88.4	54.5	1.9
SE584430-170665	Sjösafjärden	Baltic Proper	86.9	44.9	1.6
SE584420-172515	Ringsöfjärden sek namn	Baltic Proper	96.3	15.0	16.9
SE584400-172270	Dragviksfjärden	Baltic Proper	94.5	0	16.0
SE584390-172085	Kräkfjärden	Baltic Proper	96.0	0	22.0
SE584333-172895	Bergöområdet	Baltic Proper	92.5	0	17.0
SE584227-171600	Risöområdet sek namn	Baltic Proper	93.1	0.9	17.0
SE584215-170800	Aspafjärden	Baltic Proper	94.5	19.1	7.0
SE584085-171600	Örsbaken	Baltic Proper	98.4	7.9	30.0
SE584065-171200	Ålöfjärden	Baltic Proper	97.9	8.2	18.9
SE583970-170280	Marsviken	Baltic Proper	96.0	14.2	10.5
SE583900-170800	Furöområdet sek namn	Baltic Proper	92.2	0	31.0
SE583900-162500	Inre Bråviken	Baltic Proper	98.0	54.5	6.9
SE583875-170270	Sillöfjärden	Baltic Proper	96.8	16.6	17.8
SE583825-163500	Mellersta Bråviken	Baltic Proper	98.5	32.7	15.6
SE583755-163200	Ållonöfjärden	Baltic Proper	95.9	33.1	1.5
SE583730-164501	Yttre Bråviken	Baltic Proper	98.6	34.7	20.3
SE583730-162500	Svensksundsviken	Baltic Proper	97.8	19.1	2.7
SE583370-165290	Bosöfjärden sek namn	Baltic Proper	96.4	14.3	10.8
SE560205-143545	Sölvesborgsviken	Baltic Proper	97.2	0	6.0
SE560200-143175	Valjeviken	Baltic Proper	96.4	0	7.0

(*Continued*)

(*Continued*)

HID	Name	Basin	Cover (%)	BA (%)	Estimated D_{TA} (m)
SE555950-142740	Tostebergabukten	Baltic Proper	98.8	0	10.0
SE555685-142290	Landöbukten sek namn	Baltic Proper	99.6	0	11.0
SE572838-115515	Läddholmsviken	Kattegatt	93.2	0	6.0
SE572980-115576	Stallviken	Kattegatt	93.8	0	8.0
SE573044-115355	Risö-Säröarkipelagen	Kattegatt	96.6	0	14.0
SE573100-115580	Skörvallaviken	Kattegatt	88.8	0	4.0
SE573173-115587	Maleviken	Kattegatt	96.4	0	3.0
SE573322-115478	Kräklingeområdet	Kattegatt	96.2	0	14.0
SE573500-115150	Askims fjord	Kattegatt	96.5	0	25.0
SE573547-114617	Styrsö- Vrångöområdet	Kattegatt	92.2	0	23.0
SE573657-114572	Halsviken	Kattegatt	88.1	0	7.0
SE573797-114618	Brännö- Styrsöområdet	Kattegatt	89.7	0	16.0
SE573860-115000	Asperöfjorden sek namn	Kattegatt	94.0	0	22.0
SE574000-114230	Dana fjord	Kattegatt	98.0	27.2	17.8
SE574050-114780	Rivö fjord	Kattegatt	95.9	44.2	6.9
SE574330-114000	Stora Kalvsund	Skagerrak	96.1	11.9	18.5
SE574370-114250	Björköfjorden	Skagerrak	97.2	46.3	11.4
SE574630-113940	Källö fjord	Skagerrak	98.0	47.2	10.9
SE574650-114360	Nordre Älvs fjord	Skagerrak	98.4	39.0	6.2
SE574870-113795	Sälö fjord	Skagerrak	96.6	48.8	7.0
SE575340-113000	Marstrandsfjorden	Skagerrak	97.6	36.5	28.8
SE575500-113750	Älgöfjorden	Skagerrak	96.1	48.6	6.4
SE575700-114240	Hake fjord	Skagerrak	97.2	50.3	8.4
SE575747-113237	Klädesholmenområdet	Skagerrak	85.0	0.2	16.0
SE580025-113168	Skärhamnområdet	Skagerrak	88.5	8.2	13.0
SE580325-113500	Stigfjorden	Skagerrak	94.7	37.9	8.3
SE580338-112901	Kråke fjord	Skagerrak	92.8	0	28.0
SE580500-112970	Lyresund	Skagerrak	94.2	0.8	33.1
SE580500-114725	Askeröfjorden	Skagerrak	94.9	46.6	7.3
SE580530-112700	s Käringöfjorden inre skärgård	Skagerrak	94.5	22.8	10.4
SE580550-112460	Käringöfjorden	Skagerrak	98.7	0.6	31.1
SE580610-113615	Kalvöfjorden	Skagerrak	95.7	24.6	2.7
SE580650-113000	Boxvike kile	Skagerrak	73.6	24.4	–
SE580688-114860	Halsefjorden	Skagerrak	98.2	43.6	9.9
SE580765-112501	n Käringöfjorden inre skärgård	Skagerrak	93.7	4.0	11.2
SE580860-114560	Tången området	Skagerrak	92.6	0	17.0
SE581120-112680	Ellösefjorden	Skagerrak	91.6	27.4	10.1
SE581200-112960	Malö Strömmar	Skagerrak	88.9	0	13.0
SE581260-113220	Koljö fjord	Skagerrak	96.8	45.0	10.7
SE581260-115280	Ljungs kile	Skagerrak	98.8	49.6	10.5
SE581338-112332	Grundsundsområdet	Skagerrak	95.4	0	18.0
SE581365-112910	Snäckedjupet	Skagerrak	89.8	0	11.0
SE581450-113140	Nordströmmarna	Skagerrak	85.9	9.2	7.2
SE581520-113750	Borgilefjorden	Skagerrak	97.2	49.2	17.3
SE581540-114000	Kalvöfjord	Skagerrak	98.3	39.6	14.0
SE581570-113040	Getevikssund	Skagerrak	90.4	24.0	10.6
SE581700-113000	Gullmarn centralbassäng	Skagerrak	98.1	47.6	31.4
SE581740-114820	Havstensfjorden	Skagerrak	99.1	48.0	13.3
SE581748-112411	Saltö fjord	Skagerrak	96.8	15.4	21.3
SE581853-112736	Trälebergskile	Skagerrak	86.6	0	10.0
SE582000-112350	Yttre Brofjorden	Skagerrak	97.3	36.4	21.6
SE582000-115270	Byfjorden	Skagerrak	97.5	39.9	18.5
SE582040-112157	Slaholmen området	Skagerrak	90.0	0	3.0
SE582147-111771	Kungshamn s skärgård	Skagerrak	92.0	3.4	28.1

(*Continued*)

(*Continued*)

HID	Name	Basin	Cover (%)	BA (%)	Estimated D_{TA} (m)
SE582150-112530	Brofjorden	Skagerrak	95.6	35.4	12.0
SE582210-111880	Hovenäset området	Skagerrak	91.6	20.8	13.3
SE582230-112255	Åbyfjorden	Skagerrak	96.4	46.8	10.2
SE582500-113890	Saltkällefjorden	Skagerrak	96.0	57.0	12.7
SE582630-113515	Färlevfjorden	Skagerrak	95.2	52.8	7.9